

University of Nevada, Reno

Discovering the last Triassic giant: Insights from the marine Late Triassic of Nevada and a new ichthyosaur locality from New York Canyon, Nevada, USA.

A thesis submitted in partial fulfillment of the
Requirements for the degree of Master of Science
in Geology

by

Gary A. McGaughey

Dr. Paula J. Noble/Thesis Advisor

August 2023



THE GRADUATE SCHOOL

We recommend that the thesis
prepared under our supervision by

entitled

be accepted in partial fulfillment of the
requirements for the degree of

Advisor

Committee Member

Committee Member

Graduate School Representative

Markus Kemmelmeier, Ph.D., Dean
Graduate School

Abstract:

Ichthyosaurs are a large group of marine reptiles that first appeared in the Early Triassic Period and continued to be an integral part of marine ecosystems into the Middle Cretaceous Period. At the end of the Triassic, ichthyosaurs were devastated by the end-Triassic Extinction, and never again reached the giant scale or diversity of forms seen in the Triassic. The lead up to this extinction is riddled with gaps in the fossil record. The record of ichthyosaurs in Nevada ranges from the early Triassic to the first appearance of *Shonisaurus* in the latest Carnian, but the rocks of the latest Triassic have been largely underexplored.

The Pilot and Cedar Mountains, and the Garfield Hills to the South of Berlin-Ichthyosaur State Park were surveyed for vertebrates to further explore the Triassic marine rocks of Nevada. In the Pilot Mountains, nearly 30 new fossil localities were located within the lower member of the Luning Formation, which is assigned an early Norian age. Most of the material is likely referable to *Shonisaurus* and consists of partly to completely disarticulated vertebrae, rib, girdle, and limb elements, with rarer cranial material. Isolated bones from the upper member of the Luning Formation show potential for further discoveries into the middle Norian. Outside of the Pilot Mountains, additional *Shonisaurus* material was located within Luning Formation exposures in the Cedar Mountains near previously reported localities. Reconnaissance in the Garfield Hills found no vertebrate material in the Late Triassic rocks exposed there.

Moreover, a recent discovery of *in-situ* vertebrate fossils from the latest Rhaetian in New York Canyon (NYC) in the Gabbs Valley Range of Nevada, provides clear evidence of the persistence of giant ichthyosaurs into the latest Rhaetian. Previous studies

have reported isolated ichthyosaur elements from NYC, but these have never been adequately studied or described. The specimen comprises at least 17 semi-articulated ribs and two centra from a giant ichthyosaur, comparable in size and shape to the largest known examples of *Shonisaurus*. Strong controls on ammonite biostratigraphy and organic carbon isotope geochemistry confirm that this specimen is the youngest shastasaurid ichthyosaur reported to date and indicates that these giant ichthyosaurs did not go extinct during the Norian. Instead, they persisted until the end-Triassic extinction, likely perishing as a casualty of the mass extinction event.

Dedication:

I would like to dedicate this thesis to my grandma, Karen McGaughey, who was always the first to mention that at just three years old I would tell anyone who would listen that I was going to be a “pae-ee-ontologist.” I wish you could have seen me make my lifelong dream a reality.

Acknowledgements:

I would like to acknowledge and give my heartfelt thanks to my advisor Paula Noble who made this work possible. Her patience and timely advice carried me through the highs and lows of this thesis. I would also like to thank my committee members for letting my defense be a positive experience, and for your insightful comments and suggestions, thanks to you.

I would also like to thank the many collaborators I worked with on this project. Specifically, Randy Irmis was an integral part of nearly every part of this project, providing advice and many days spent in the field. Additionally, Tylor Birthisel, Carrie Levitt-Bussian, and the rest of the staff at the Natural History Museum of Utah were most generous in providing the use of their lab spaces and materials and assisting in the field. Lastly, my New York Canyon experts: Kathleen Ritterbush, Lydia Tackett, and Montana Hodges were essential in creating a full understanding of the geology around the quarry.

I further want to thank the wonderful team of volunteers that helped in the field and in the lab. Forrest and Nadine Fasig deserve special recognition for their support in the field, providing food and transportation, and finding the fossil that the thesis is based around. I also want to recognize Saige Howard, who spent many hours in the field and especially in the lab collecting and processing samples for carbon isotope geochemistry.

Finally, I want to give special thanks to my wife Victoria and my family as a whole for their continuous support and understanding when undertaking my research and writing my thesis. I would not have been able to complete this project without their support.

Table of Content

Abstract:	i
Dedication:	iii
Acknowledgements:	iv
List of Tables:	viii
List of Figures:	ix
I. Introduction:	1
Triassic Ichthyosaur Evolution:	1
The End-Triassic Extinction:	5
Cause and Impact:	5
Carbon Isotope Record:	7
Research Objectives:	8
II. Walker Lake Terrane ichthyosaur distribution	10
Introduction:	10
Geological Setting:	10
Initial Work:	18
Objectives and Field Strategies:	19
Materials and Methods:	20
Results:	21
Garfield Hills:	21
Cedar Mountains:	21
Pilot Mountains:	23
Discussion:	24
Ichthyosaur Abundance in the Luning Formation:	24

The Upper Carbonate Member of the Luning Formation:.....	25
The Pamlico Formation:	26
III. New York Canyon Ichthyosaur	27
Objectives and Significance:	27
Materials and Methods:.....	29
Geological Setting:	29
Ferguson Hill stratigraphy:	31
Materials and Methods:	33
Results:	36
Field observations of quarry stratigraphy and structural geology:.....	36
Thin section analysis:	37
Invertebrate collections:.....	37
Carbon isotope data:	41
Vertebrate collections:.....	41
Histology:.....	42
Discussion:	43
Geological interpretations:.....	43
Proximity to the ETE.....	47
Taxonomic interpretations:	48
Systematic Paleontology:	51
IV. Conclusions:	57
V. Future Work.....	58
VI. References	59
Appendix 1	69

Appendix 2:75

List of Tables:

- Table 1. Pilot Mountains Specimen Inventory
- Table 2. Organic Carbon Isotope Results
- Table 3. New York Canyon Specimen Inventory
- Table 4. Rib Diameter Measurements

List of Figures:

- Figure 1. Ichthyosaur Phylogeny
- Figure 2. CAMP Map
- Figure 3. Regional Map of the Luning Formation
- Figure 4. Pilot Mountains Stratigraphy
- Figure 5. Pilot Mountains Geologic Map
- Figure 6. Cedar Mountains Geologic Map
- Figure 7. Northeastern Garfield Hills Geologic Map
- Figure 8. Select Field Photos from Pilot Mts. and Cedar Mts.
- Figure 9. NYC Geologic Map
- Figure 10. Annotated Quarry Photograph
- Figure 11. Petrographic Thin Sections
- Figure 12. Quarry Stratigraphy and Geochemistry
- Figure 13. Quarry Map
- Figure 14. New York Canyon Quarry Photos
- Figure 15. Rib Schematic
- Figure 16. Bone Histology Photomicrographs
- Figure 17. Ammonite Biozones
- Figure 18. Plate of ammonites

I. Introduction:

Triassic Ichthyosaur Evolution:

The world's marine ecosystems were devastated at the end of the Permian, and this devastation opened the door for multiple lineages of reptiles to enter the marine habitat, leading to the explosive radiation of marine reptiles in the Early Triassic to early Middle Triassic (Motani, 2009; Kelley and Pyenson, 2015; Moon and Stubbs, 2020). Early marine reptiles filled ecological roles that had previously never been exploited by tetrapods and set the scene for a marine ecosystem resembling the modern oceans (Stubbs and Benton, 2016). Radiation mostly occurs in two major lineages of marine reptiles, the sauropterygians (plesiosaurs and placodonts) and the ichthyosaurs, which are the subject of this study (Kelley and Pyenson, 2015). Ichthyosaurs are secondarily aquatic reptiles that are known from the Early Triassic to early Late Cretaceous (McGowan, 1991; Motani et al., 1996). The clade is known for the fish-shaped body profiles seen in its derived members. The group has a rich history in the sciences and has been known for over 200 years with numerous localities widely distributed all over the world. The generalized ichthyosaur body plan includes numerous extreme modifications of the basic reptilian skeletal design, which allowed them to adapt to a marine lifestyle and become the dominant predator of the marine ecosystem for portions of the Mesozoic.

Ichthyosaurs evolved possibly as early as the Permian Period with first appearances in the early Triassic (Kear et al., 2023). The first ichthyopterygians, including examples like *Chaohusaurus* and *Utatsusaurus* (Grippioidea), had a lizard-like body shape and likely employed an anguilliform swimming style (Motani, 1997). The early ichthyosaurs colonized the open ocean and evolved rapidly in the early Triassic

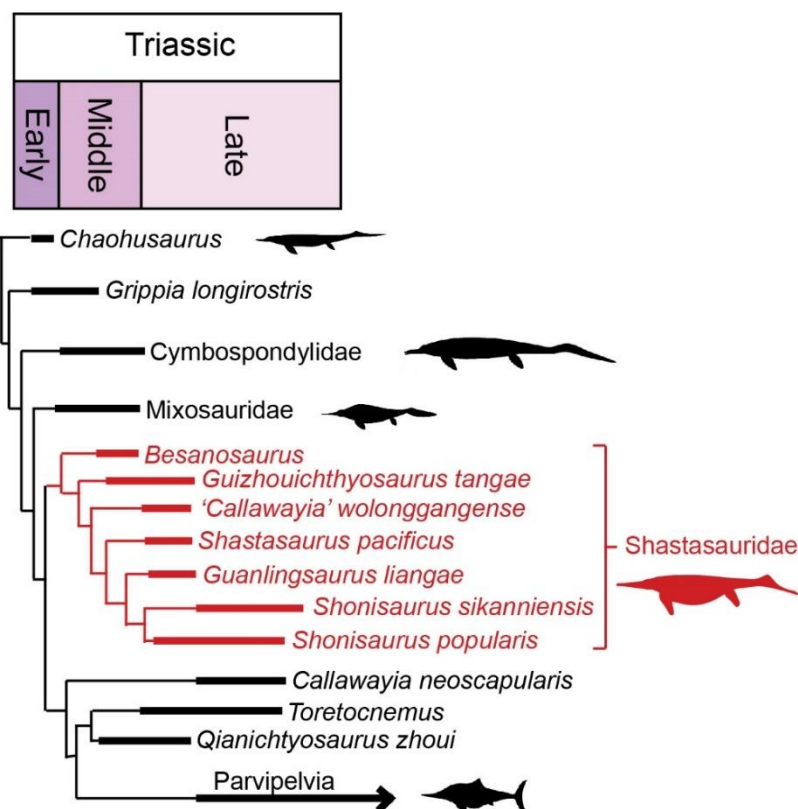


Figure 1: Triassic ichthyosaur phylogeny focusing on the Late Triassic shastasaurids. Cymbospondylidae represents the first truly giant ichthyosaurs while still retaining a lizard-like form. Mixosauridae are small ichthyosaurs that begin to develop more of the dolphin-like body plan seen in more derived ichthyosaurs. Shastasauridae contains the largest ichthyosaurs and continues the trend of developing the dolphin-like body plan seen in mixosaurs and more derived ichthyosaurs. Parvipelvia are the only clade to survive the end-Triassic extinction and develop the familiar dolphin-like shape ichthyosaurs are known for. Parvipelvians are largely deep-sea specialists with far less ecological disparity than the pre-Jurassic ichthyosaurs. Modified from Ji et al., 2016. Silhouettes modified from McGowan and Motani (2003) and Kelley (personal communications).

(Fig. 1), filling a variety of ecological niches, and colonizing the open ocean (Dick and Maxwell, 2015; Moon and Stubbs, 2020). Their colonization of the open ocean allowed them to disperse across the globe and explains their occurrence throughout the northern hemisphere. The global distribution and diverse morphology of the early ichthyosaurs made them a key component of the formation of complex multilevel ecosystems quickly after the end-Permian mass extinction (Chen and Benton, 2012; Motani et al., 2017; Sander et al., 2021). Similarly, ichthyosaur body size tells a story of rapid change as they increased in body size exceptionally fast. The family Cymbospondylidae evolved giant

forms with a skull length of 2 m by the early middle Triassic, less than 5 Ma after their first appearance (Sander et al., 2021). Simultaneously, in Mixosauridae we begin to see a transition to the fish-like body plan, including the development of a dorsal fin that is likely to accompany the adoption of thunniform swimming, the swimming mode seen in tunas and other marine vertebrates capable of high-speeds and long distance (Renesto et al., 2020).

While the large-bodied ichthyosaur family Cymbospondylidae was on the rise, another group of medium to large-bodied ichthyosaurs, the Shastasauridae, made their first appearance. Shastasauridae are an intermediate group in Ichthyosauria that retains some of the more lizard-like features of the basal members of the clade, including a relatively robust pelvic girdle and a long slender body (McGowan and Motani, 1999; Nicholls and Manabe, 2004). Members of this clade ranged in size from a moderate 6 m all the way to the largest of the known ichthyosaurs, a whale-sized giant named *Shonisaurus sikanniensis* that was roughly 21 m long (Nicholls and Manabe, 2004). The monophyly of Shastasauridae has been debated, and it has been recovered as a paraphyletic group by several publications (e.g. Sander et al., 2011; Moon and Stubbs, 2020). Here, I will be using the node-based definition from Ji et al. (2016), comprising the last common ancestor of *Shastasaurus* and *Besanosaurus*, and all its descendants. Currently, this includes five valid genera: *Shastasaurus*, *Besanosaurus*, *Guanlingsaurus*, *Guizhouichthyosaurus* and *Shonisaurus* along with a species of uncertain generic assignment '*Callawayia*' *wolonggangense* (Fig. 1).

The Late Triassic ichthyosaurs of Nevada present a variety of opportunities for continuing research, including understanding their paleoecology, distribution, and

evolutionary patterns in response to mass extinction events. Berlin-Ichthyosaur State Park (BISP) has been at the forefront of many of these research questions and is one of the most researched active areas of study in regards to a konzentrat-lagerstätten (well-preserved high density bed) displayed in the BISP visitor's, and its potential causes. First discovered in 1928 by Simeon Muller, BISP was actively excavated by Charles Camp and others at UC Berkeley's Museum of Paleontology (UCMP) from 1954 through 1965. Over this time at least 37 individuals from 10 quarries were identified in the upper Luning Formation spanning the latest Carnian-early Norian. Many hypotheses have been proposed to explain the perceived mass mortality displayed in the main fossil shelter at BISP (Camp's Quarry 2) including a mass beaching event or a deadly algal bloom (Hogler, 1992). These hypotheses are not supported by geologic or taphonomic evidence however, and instead the concentration is more likely a representative sample of the high population of these ichthyosaurs that were living in this area for part of their lifecycle (Kelley et al. 2022). The high concentration of *Shonisaurus* remains at BISP stands out because the faunal assemblage is monotaxic and consists almost entirely of adults and some embryonic material (Camp 1980, Kelley et al., 2022). Kelley et al. (2022) explained the odd community structure at BISP as a potential breeding ground, but the Luning Formation is not limited to BISP, and it remains uncertain if the community structure seen at BISP is present in the other mountain ranges where the Luning Formation outcrops. Large ichthyosaur remains are repeatedly noted south of BISP in both the Pilot and Cedar Mountains (Camp, 1980; Firby et al., 1981; Balini et al. 2014), but no follow-up work has been done on the ichthyosaur remains reported at these sites, and they were the initial focus of this project.

Triassic ichthyosaurs were quite diverse and rapidly evolved a variety of feeding strategies and body sizes (Ji et al., 2016). Many types of dentition evolved in ichthyopterygia during the Triassic, indicating the widest range of trophic adaptations within this group (Motani, 2005). Throughout the entirety of the Triassic, ichthyosaurs appear to dominate the world's oceans with high diversity and disparity (Thorne et al., 2011; Fröbisch et al., 2013; Kelley and Pyenson, 2015). The end of the Triassic, however, marked an end to their ecological dominance. The end-Triassic mass extinction (ETE) caused a major evolutionary bottleneck in ichthyosaurs and only a single group, the parvipelvians, survived into the Jurassic. Ichthyosaur diversity would return to pre-extinction levels in the Early Jurassic, but the disparity of forms and niches would remain greatly reduced (Thorne et al., 2011; Moon and Stubbs, 2020). Additionally, the rate of evolution in Ichthyosauria would reduce significantly and remain reduced throughout the rest of the clade's 100 million year existence (Moon and Stubbs, 2020).

The End-Triassic Extinction:

Cause and Impact:

The Triassic Period ended with a major mass extinction event, the ETE. Considered one of the big five extinction events, it is marked by significant increases in extinction rates of marine fauna, and well documented turnovers in terrestrial vertebrate groups and vegetation (Benton, 1995; Guex et al., 2004; van de Schootbrugge et al., 2009; Alroy, 2010). The ETE occurred ~201.51 million years ago and was caused by major volcanic activity during the break-up of the supercontinent Pangea (Blackburn et al., 2013; Percival et al., 2017; Davies et al., 2017). This volcanic activity emplaced the

central Atlantic magmatic province (CAMP), one of the most expansive large igneous provinces (LIP) in the world, covering an area of $\sim 107 \text{ km}^2$ (Fig. 2) (Whiteside et al., 2010; Blackburn et al., 2013). Greenhouse gas emissions from the emplacement of CAMP basalts are considered the primary trigger for the environmental changes associated with the biotic loss at the end-Triassic (Thibodeau et al., 2016; Zaffani et al., 2018). The associated rapid rise in atmospheric CO_2 is linked to climatic perturbations that initiated global warming, ocean acidification, and ocean anoxia (Greene et al., 2012; Pálffy and Kocsis, 2014; Atkinson and Wignall, 2019).

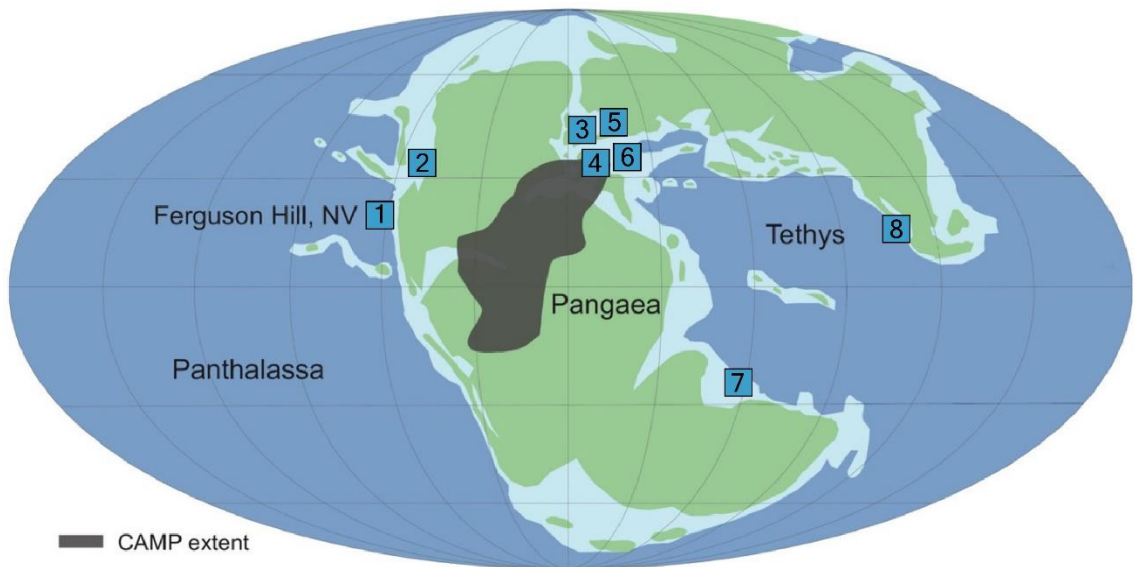


Figure 2: Paleogeographic map of the Latest Triassic/Early Jurassic showing the extent of CAMP volcanism. Markers note the location of known Late Triassic ichthyosaur localities. 1 = New York Canyon/Ferguson Hill Nevada, BISP, and other Nevada localities (Camp, 1980; Kelley et al., 2022); 2 = British Columbia (Nicholls and Manabe, 2004); 3 = United Kingdom (Lomax et al., 2018); 4 = Southern France (Fischer et al., 2014); 5 = Germany (Sander et al., 2016); 6 = Swiss Alps (Sander et al., 2021); 7 = Tibet and Southern China (Motani et al., 1999); 8 = Guanling, China (Yin et al., 2000). Modified from Larina et al. (2021).

In the marine record there is a notable loss of ammonoids and a devastation of the scleractinian corals (Guex et al., 2004; Alroy, 2010). Conodonts, an important index fossil, are completely wiped out by the ETE, though they had already been severely reduced in diversity by the Norian (Tanner et al., 2004). The marine record also records a

significant evolutionary bottleneck for the ichthyosaurs, which reduced the important group of marine tetrapods to just three or four lineages (Thorne et al., 2011; Moon and Stubbs, 2020). The terrestrial ecosystem was just as impacted and ETE is recognized by a turnover in sporomorphs, megafloora, and early Mesozoic vertebrates on land (Benton, 1995; McElwain et al., 1999, 2009; van de Schootbrugge et al., 2009).

Carbon Isotope Record:

Carbon isotope records have been used as the primary linkage between CAMP volcanism, increased atmospheric CO₂, and the ETE. Global studies on marine organic carbon isotope records have recognized three negative carbon isotope excursions (CIEs) that are associated with the emplacement of CAMP, referred to as the “main”, “initial”, and “precursor” CIEs (Ruhl and Kürschner, 2011). These have been hypothesized to be correlated to multiple disruptions in the global carbon cycle around the ETE that led to the release of ¹³C-depleted carbon marking these negative excursions (Thibodeau et al., 2016; Fujisaki et al., 2018; Korte et al., 2018; Heimdal et al., 2020). The precursor CIE has been documented in shallow marine sections from the Tethys (Ruhl and Kürschner, 2011; Corso et al., 2014; Zaffani et al., 2018) and in the deep marine of the Panthalassic Ocean (Fujisaki et al., 2020). This precursor CIE is shorter in duration and smaller in magnitude when compared to the initial carbon isotope excursion (ICIE), but it could be linked to an early phase of CAMP emplacement that perturbed the global carbon cycle (Larina et al., 2021). In eastern Panthalassa, this perturbation coincides with reduced diversity in the shallow marine ecosystem that included taxa tolerant to low oxygen

levels and reflected deteriorating conditions that led to ecosystem collapse during the main phase of CAMP (Larina et al., 2021).

The ICIE is considered the onset of the ETE and is documented worldwide in terrestrial and marine environments (Corso et al., 2014; Yager et al., 2017; Korte et al., 2018; Ruhl et al., 2020). The cause of the release of ^{13}C -depleted carbon has been attributed to multiple sources including volcanic emissions from CAMP basalts (e.g., Pálffy and Kocsis, 2014; Corso et al., 2014; Thibodeau et al., 2016), release from marine methane clathrates due to a warming climate (Korte et al., 2018), and thermogenic methane derived from organic-rich sediments released by intrusive CAMP activity (Ruhl and Kürschner, 2011; Davies et al., 2017; Heimdal et al., 2020). In marine environments, the ICIE occurs alongside the last occurrence (LO) of *Choristoceras crickmayi*, the last Triassic ammonoid in North America (Guex et al., 2004), in the Northern Calcareous Alps a similar relationship is observed but with *Choristoceras marshi* (Ruhl et al., 2009). Thus, a detailed framework is provided for a high-precision correlation around the globe. However, not all CIEs around the Late Rhaetian are attributed to global factors, the negative organic CIE in the Bristol Channel (UK) has been argued to be the result of a transition from marine to nonmarine conditions.

Research Objectives:

The aim of this study is to determine the upper stratigraphic limit of shastasaurid ichthyosaurs in Nevada. At BISP, *Shonisaurus* is known from the Late Carnian, but a large vertebrate fossil from the early Norian strata of the upper carbonate member of the Luning Formation may be referable to the genus as well. Similarly, in the Pilot

Mountains large ichthyosaur material is noted only as recently as the early Norian, and prior to this study relative abundance compared to BISP was unknown. There are a few possible explanations for this apparent disappearance of large ichthyosaurs. The Late Triassic was a time of relative biological turmoil and a variable climate (Trotter et al., 2015). A global humid episode known as the Carnian Pluvial Event starts at the boundary between the upper and lower Carnian and was followed by further climatic perturbations at the Norian/Rhaetian boundary (Rigo et al., 2007, 2020). As such, these climatic perturbations may have caused a regional extinction of large ichthyosaurs. The disappearance may also be linked to less catastrophic causes as we see facies changes in the Late Triassic marine strata of Nevada (Muller and Ferguson, 1936). The depositional environments of Nevada from the middle Norian through the Rhaetian may have been a less ideal habitat for these ichthyosaurs, leading to their disappearance from the fossil record. Globally, the extinction of large shastasaurids is likely linked to the ETE. Partial remains from the Rhaetian in Europe demonstrate that large ichthyosaurs survived into the final stage of the Triassic in the Tethys and seem to disappear before the beginning of the Jurassic (Callaway and Massare, 1989; Fischer et al., 2014; Lomax et al., 2018; Sander et al., 2022).

In order to clarify the stratigraphic extent of large shastasaurids in Nevada and explore the upper stratigraphic extent of shastasaurids globally this thesis focuses on two research areas: the Luning-Berlin Assemblage in the Pilot and Cedar Mountains and the Triassic/Jurassic sequence in the Gabbs Valley Range. The Luning Formation in these mountain ranges is similar to its presentation at BISP, but in this area it is divided into different members than those seen at BISP, and it is slightly younger than BISP. The

sequence in the Gabbs Valley Range covers the Latest Triassic into the Jurassic and includes evidence of the ETE. Both sites have been noted to contain ichthyosaur material, but the extent and taxonomy of the material is relatively undescribed (Muller and Ferguson, 1936; Laws, 1982; Lucas et al., 2007; Taylor et al., 2000). The study aims to thoroughly survey these two areas, confirm the presence or absence of ichthyosaur remains, and more precisely identify the ichthyosaurs present.

II. Walker Lake Terrane ichthyosaur distribution

Introduction:

Geological Setting:

The Walker Lake terrane is composed of Triassic-Jurassic carbonate, siliclastic, volcanic, and volcanoclastic rocks in Southwestern Nevada (Silberling, 1991; Crafford, 2007). This terrane is divided into three structurally bounded allochthonous assemblages: the Pine Nut, Pamlico-Lodi, and Luning-Berlin assemblages. These assemblages are stratigraphically similar, and the Pamlico-Lodi and Luning-Berlin assemblages share similar multiphase structural histories (Oldow, 1984; Crafford, 2007). Together these assemblages form an accretionary complex of Triassic volcanogenic rocks interfingering and overlain by a Late Triassic-Early Jurassic carbonate platform that grades into terrigenous clastic and volcanogenic rocks (Silberling, 1991). The bulk of the Triassic rocks from these assemblages are assigned to the Luning and Pamlico Formations.

The Luning Formation is a mixed carbonate-siliclastic unit containing calcareous shales and argillites, clastic rocks, dolomites, and limestones. The Luning Formation is exposed in the Pilot Mountains, Shoshone Mountains, Gabbs Valley Range,

Cedar Mountains, and Paradise Range (Fig. 3). The unit varies in thickness from 1-2.8 km depending on location and the base of the formation is a fault contact in all but the Shoshone Mountains where it unconformably overlies the Middle Triassic Grantsville Formation (Silberling, 1959; Oldow, 1981). In the Pilot Mountains the structure of the Luning Formation is further defined as an allochthonous series of four thrust nappes that have undergone multiple phases of Mesozoic contractional deformation (Oldow, 1981). The stratigraphy varies among the localities, seeming to fall into two categories: those most similar to the Shoshone Mountains stratigraphy and those most similar to the Pilot Mountains stratigraphy. The stratigraphy and depositional environment of the Luning Formation in these ranges differs fundamentally (Fig.4). In the Shoshone Mountains, the formation is considered to represent a deeper water facies than in the Pilot mountains, lacking the reef buildups present in the Pilot Mountains (Silberling, 1959; Stanley, 1979; Fucelli et al., 2023). In the Shoshone Mountains, the Luning Formation has been divided into four informal members in ascending order: clastic, shaly limestone, calcareous shale, and carbonate (Silberling, 1959). The Pilot Mountains stratigraphy is divided into only three informal members: lower carbonate, middle clastic, and upper carbonate (Silberling, 1959) (Fig. 5). The Cedar Mountains are most similar to the Pilot Mountains in stratigraphy, but in the Cedar Mountains the middle member is further subdivided into a middle clastic member and a middle shaly member (Fig. 6) (Brown, 1986).

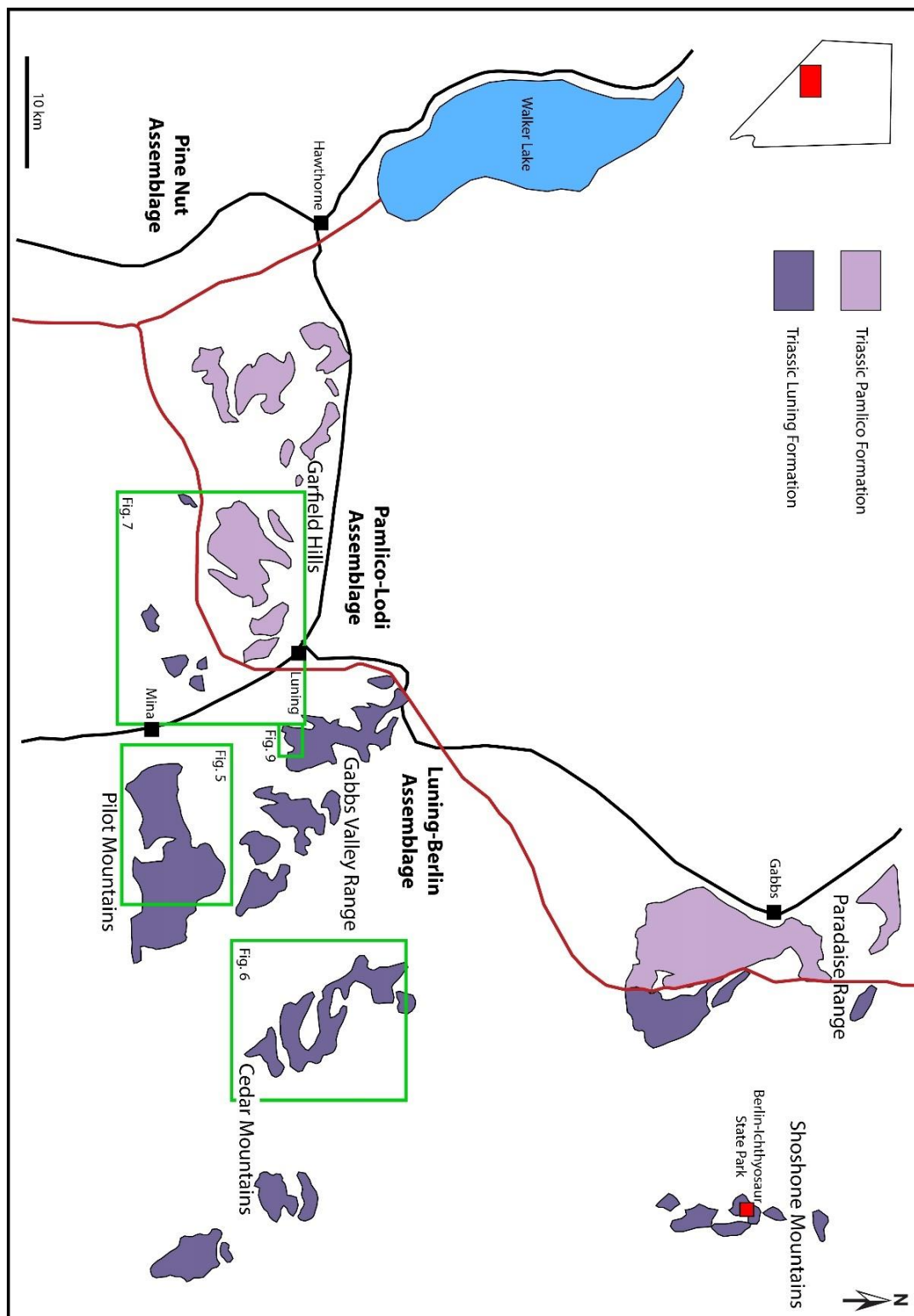


Figure 3: Regional Map of the Luning Formation and age-equivalent Pamlico Formation in the Walker Lake terrane. The formations are differentiated based on the higher volcanoclastic component of the Pamlico Formation and the position of the two formations in different thrust assemblages (Ferguson and Muller, 1949; Oldow, 1981; and Oldow et al., 1993). Higher resolution geologic maps are highlighted in green boxes.

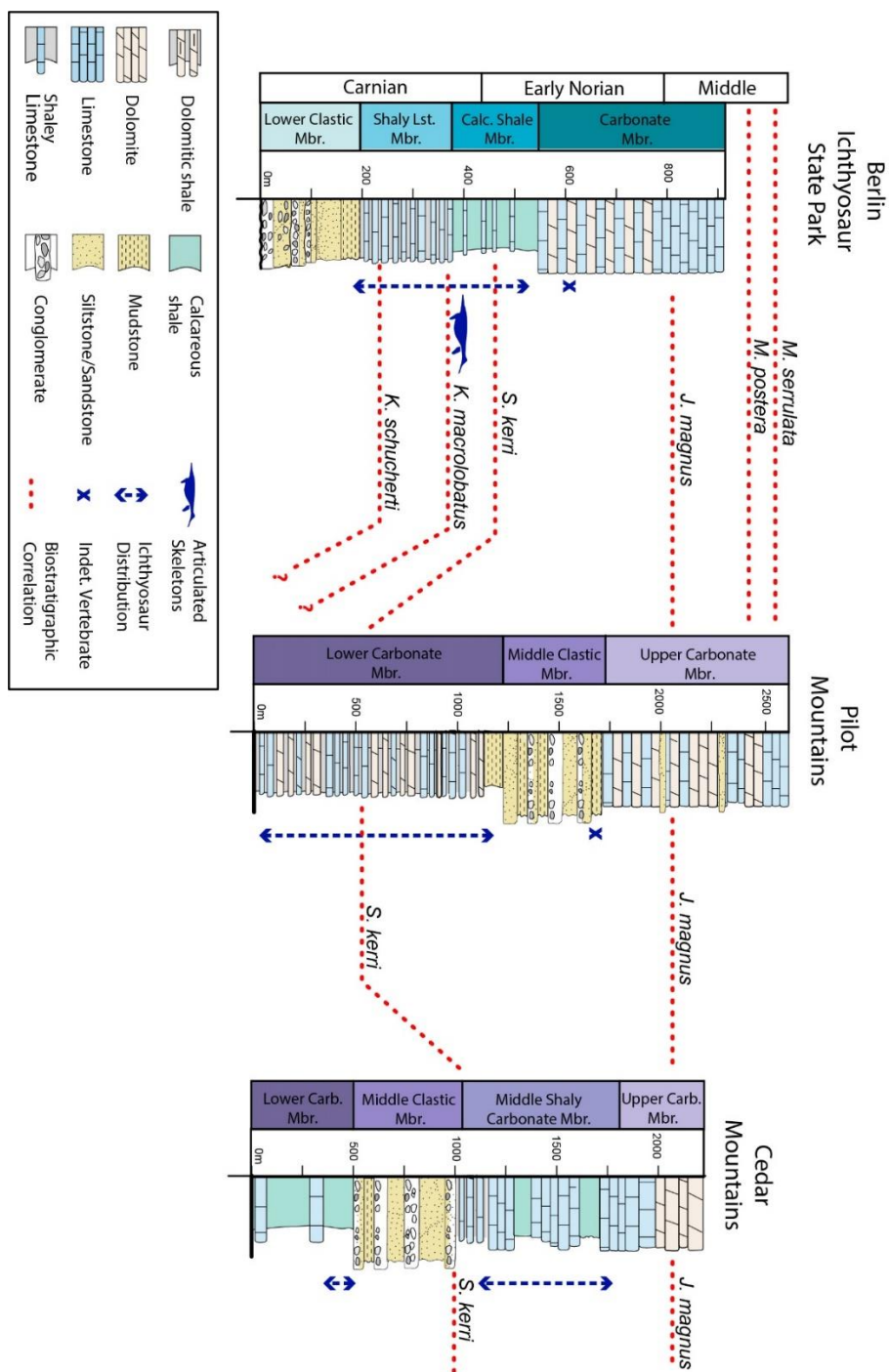


Figure 4: Generalized stratigraphy of the Luning Formation in Nevada. The stratigraphy of the Pilot and Cedar Mountains is notably similar, though the middle member can be split into two separate members in the Cedar Mountains. The stratigraphy in the Shoshone Mountains differs in both age and position of the clastic member relative to the other lithostratigraphic members. *Mockina postera* and *M. serrulata* are conodont biozones indicative of the Middle Norian (Fucelli et al., 2023). Biostratigraphic index ammonite *Juvavites magnus* serves as the reference datum for correlation (Oldow et al., 1993; Martindale et al., 2012; and Kelley et al., 2022). Lithostratigraphic member color scheme for BISP from Kelley et al. (2022).

(38° 25' 17.49" N, 118° 5' 30.92" W)

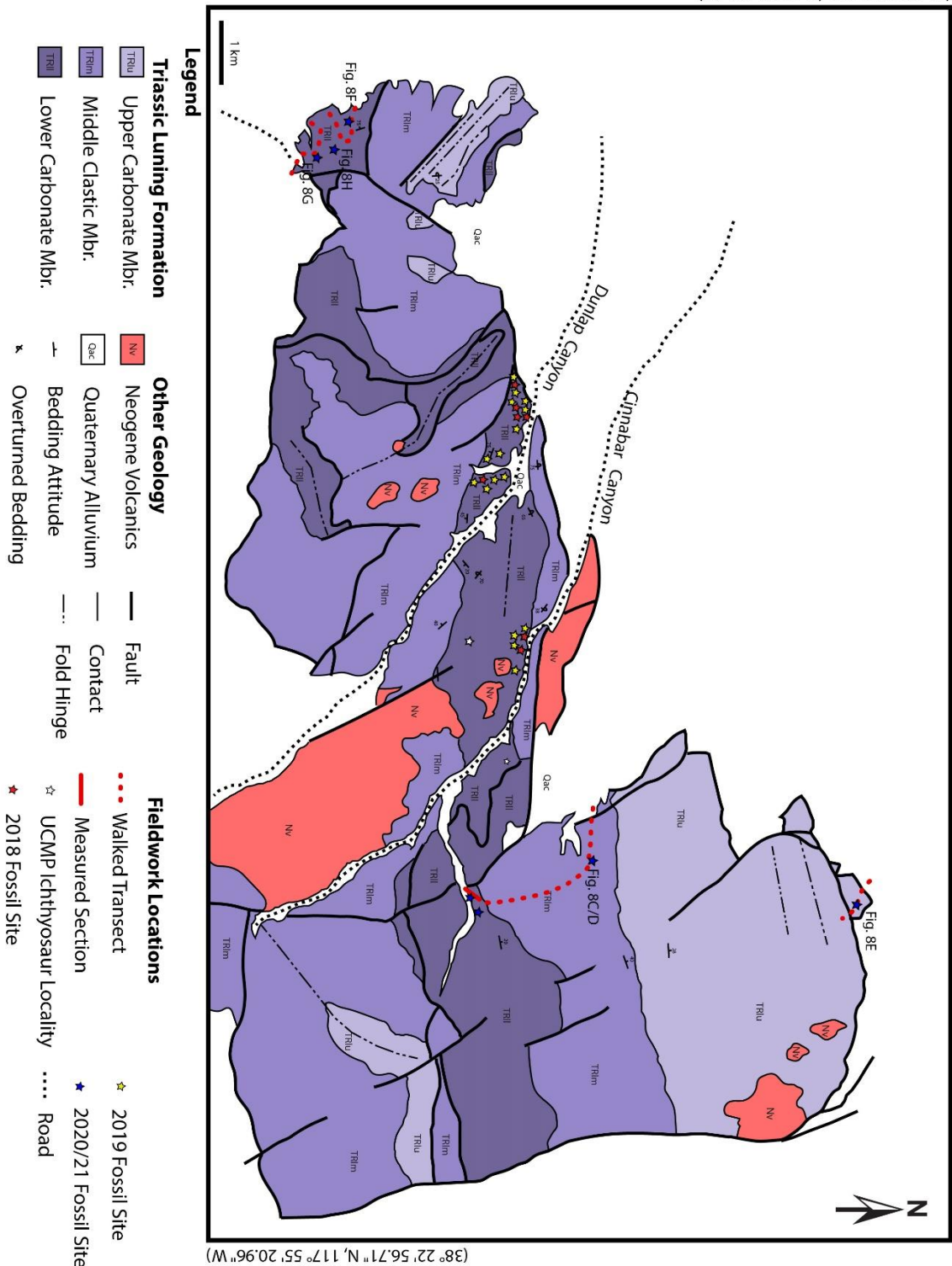


Figure 5: Simplified geologic map of the Triassic strata on the northern slope of the Pilot Mountains. The type section of the Luning Formation is present on the right side of the map and extends from near the beginning of the measured section North through the middle and upper members of the unit. From Oldow and Meinwald (1992) and Oldow and Dockery (1993).

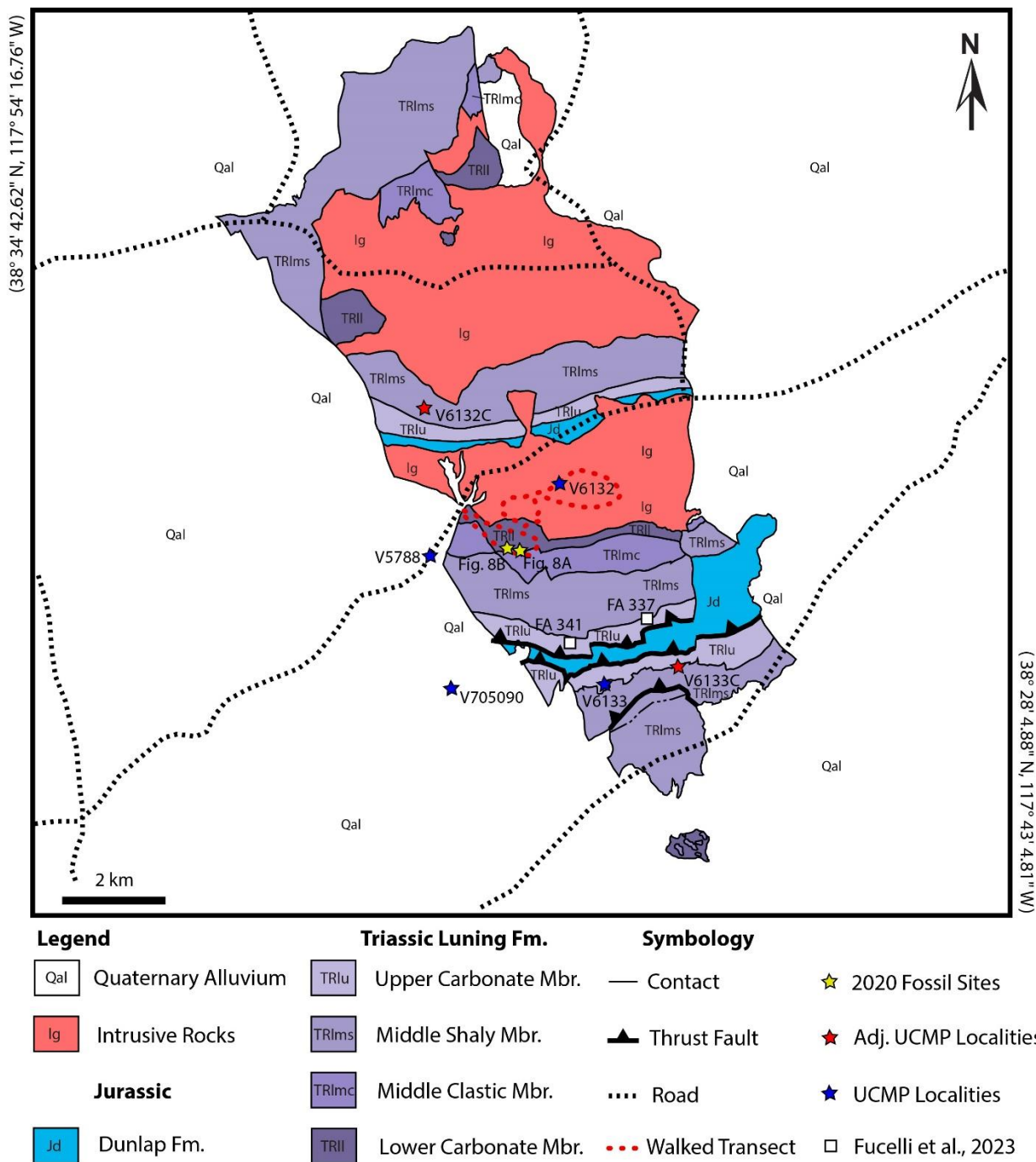


Figure 6: Simplified geologic map of the Cedar Mountains. Blue stars show the locations of known UCMP localities from James Firby's Paleontological Resources Inventory (Firby, 1981). Personal observations proved these coordinates to be inaccurate. Red stars show the approximate location of the corrected position of two of these localities based on field notes from S.D. Webb, 1961 and J.E. Mawby (1961). Fucelli et al., 2023 localities are for invertebrates. Modified from Ferguson and Muller (1949) and Brown (1986).

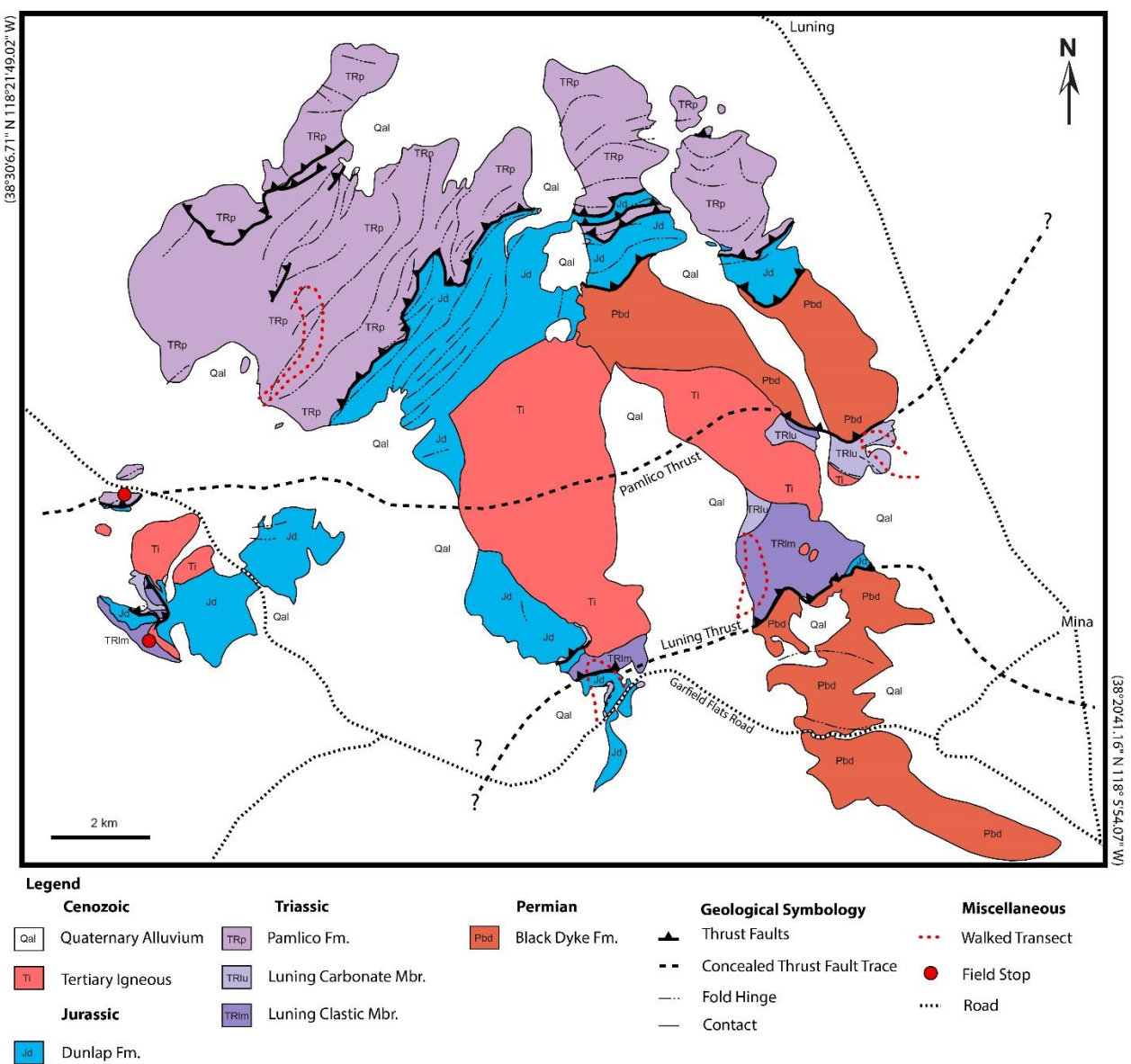


Figure 7: Simplified geologic map of the Northeastern Garfield Hills. The Pamlico Formation and Luning Formation are considered chronologically equivalent, though biostratigraphic dating in the Pamlico has not been done. The Pamlico Thrust separates the two equivalent units. Subdivision of the Pamlico Formation into members was only done in the western Garfield Hills. Modified from Ferguson and Muller (1949), Oldow (1978), and Oldow (1981).

Another important difference is that in the Shoshone Mountains, the base of the formation is older than the type locality in the Pilot Mountains, extending down into the Late Carnian *schucherti* and *macrolobatus* ammonite biozones. In the Pilot Mountains, the base of the Luning Formation is structural and biostratigraphic age constraints place the lower carbonate member of the Luning Formation in the early Norian *kerri* Zone; the

base of the upper carbonate member has yielded lower middle Norian ammonoids of the *magnus* zone (Oldow, 1981; Sandy and Stanley, 1993). Conodonts from the upper carbonate member push the age even younger with species of the *Mockina postera* and *Mockina serrulata* zones placing the member firmly in the middle Norian (Fucelli et al., 2023). The vertebrate fossil bearing rocks in the Shoshone Mountains range from the Carnian *schucherti* Zone up through the Norian *kerri* Zone, with the highest abundance occurring in the Latest Carnian *macrolobatus* Zone. Whereas, in the Pilot Mountains all the known vertebrate fossil bearing rocks occur in the *kerri* Zone. The general chronology is similar to that of the Pilot Mountains, but some of the thrust nappes do contain fossils of a Late Carnian age similar to what is recorded in the Shoshone Mountains (Brown, 1986).

The Luning Formation is seen in the southeastern Garfield Hills, but the coeval Pamlico Formation makes up the majority of the Triassic outcrops in the region (Fig. 7). Previous work had mapped the unit as both the Luning and Excelsior Formations (Ferguson and Muller, 1949). The Pamlico Formation is the primary component of the Pamlico Allochthon that structurally overlies the Luning Allochthon (Oldow, 1978). The Pamlico Formation is lithologically distinct from the Luning and Excelsior formations and consists of intermediate to felsic volcanic rocks, volcanoclastic rocks, and carbonate rocks (Oldow, 1978). The Pamlico Formation was deposited in a shallow marine and near-source subaerial environment that has been interpreted to be from near a volcanic archipelago (Oldow, 1978). In the western Garfield Hills, the Pamlico Formation can be subdivided into three informal members. A lower member consisting of thick carbonate and volcanogenic units of equal parts volcanic and volcanoclastic rocks. A middle

member of locally fossiliferous carbonate rocks and volcanogenic units dominated by volcanoclastic sedimentary rocks, and an upper member primarily composed of massive crystalline limestone (Oldow, 1978).

The first ichthyosaur fossils from the Pilot Mountains were discovered in 1929 and 1930 by Siemon Muller, who found large ichthyosaur remains in both the Pilot and Shoshone Mountains (Camp, 1980). Muller collected a single femur from Dunlap Canyon in the Pilot Mountains that was later assigned to the species *Shonisaurus mulleri* by Camp (1980). In the late 1970's large ichthyosaurs were reported across all facies in the lower member of the Luning in the Pilots and a UC Berkely Museum of Paleontology (UCMP) locality was recorded in Cinnabar Canyon (Fig. 5) (Cornwall, 1978). In the Cedar Mountains, four UCMP vertebrate localities are listed in their records (Fig. 6). Field notes in the UCMP archive by S.D. Webb and J.E. Mawby in 1961 list Hugh Mottern as the first person to discover ichthyosaurs in the Cedar Mountains. The material is described as primarily vertebrae and ribs with some larger bones and plentiful fragments.

Initial Work:

Vertebrate fossils reported in Dunlap and Cinnabar canyons in 2018 by two members of the public, Forrest and Nadine Fasig. Further investigation identified the specimens as *Shonisaurus* and noted a relatively high abundance of bone in the area. In the Spring and early Summer of 2019, additional surveying in the area determined that the lower Luning Formation in both Dunlap and Cinnabar canyons contains abundant ichthyosaur remains (Fig. 5), the majority of which may be assigned to *Shonisaurus*,

based on their large size and gross morphology. The material found *in-situ* was associated with shaly facies interbedded with coarser fossiliferous limestone. In some cases, bone was found *in-situ* within bioclastic beds. The material was largely disarticulated, but some of the localities appear to be semi-articulated and may have potential for future excavations.

Objectives and Field Strategies:

Given the volume of *Shonisaurus* material in the Luning Formation of the Pilot and Shoshone mountains, it was determined that further exploration of the Luning and the equivalent Pamlico Formation would be useful in determining the extent of *Shonisaurus*. Outside of further exploration of the Luning Formation in the Pilot Mountains, the Luning Formation had been mapped in the Cedar Mountains to the East and this range was already known to contain ichthyosaurs, based on three UCMP localities. Exploration of the Pamlico was limited to the eastern Garfield Hills. Thus, in summary, the goals for the initial field season were to relocate the UCMP localities in the Cedar Mountains, survey the Luning in both the Pilot Mountains and the Cedar Mountains to determine the abundance and stratigraphic distribution of ichthyosaur material in the Luning Formation, and to conduct initial surveys for ichthyosaur material in the Pamlico Formation of the Garfield Hills.

Following initial exploration in the first field season, the Luning Formation in the Pilot Mountains was selected for more in-depth analyses, and reconnaissance was extended to the Gabbs Valley Range (see chapter II). The goal of this was to determine the upper stratigraphic limit of large shastasaurid ichthyosaurs from the type locality of

the Luning, including the lower and upper members. In addition, bulk samples would then be taken for microvertebrate processing to better constrain the community structure of the lower member and determine if there was a significant change that could be linked to the disappearance of these large apex predators.

Materials and Methods:

Field investigations focused on the type locality of the Luning Formation in the Pilot Mountains of Nevada. Additional field investigations encompassed the Garfield Hills to the West of the Pilot Mountains and the Cedar Mountains to the East. At all localities, fieldwork began with scouting for vertebrate material along transects through marine Triassic strata and relocating UCMP localities reported from both the Cedar and Pilot Mountains. New fossil localities were marked with a GPS point and given a field number; photographs were also taken of *in-situ* material. Fossil collections were not made in either the Garfield Hills or the Cedar Mountains.

In the Pilot Mountains transects were undertaken through the lower and upper members of the Luning Formation to look for bone abundance, and additional focus was given to the lower member as a pilot survey for microvertebrate faunas. A section at the top of lower member of the Luning Formation at its type locality (Fig. 5) was measured and sampled. The section was measured using the Jacob's Staff design from Holland and Regan (2020). Hand samples were etched in the field using diluted acetic acid and examined for microfossils. Bulk samples for microfossil processing were chosen based on stratigraphic position and perceived potential. Microfossils were extracted using a buffered acetic acid process.

Results:Garfield Hills:

Scouting in the Pamlico/Luning Formation of the Garfield Hills recovered sparse invertebrate fossils, and no vertebrate remains along the walked transects and short vehicle stops (Fig. 7). Gastropods and bivalves were observed in some units, but these were in considerably lower abundance than what is observed in either the Cedar or Pilot Mountains. The Triassic marine strata in the Garfield Hills were folded and altered to a greater extent than what was observed in the other two ranges.

Cedar Mountains:

In the Cedar Mountains, the given coordinates for the UCMP ichthyosaur localities in the were inaccurate and led to points in intrusive igneous rocks (V6132) and in the alluvium (V5788 and V705090) (Fig. 6). A transect walked through rocks mapped as the Luning Formation by Ferguson and Muller (1949) did locate large ichthyosaur fossils. At this site large ichthyosaur fossils that are likely of the genus *Shonisaurus* were relatively abundant both *in-situ* and in float (Fig. 8A-B). The vertebra is characteristically large in diameter and antero-posteriorly short. The *in-situ* fossils were found in a fissile shale matrix underlying a more resistant bioclastic bed. The fossils at this locality all exhibited a characteristic red/purple coloration that was not seen at any of the other Luning Formation localities (Fig. 8A-B). Bivalves were abundant throughout the area around the locality. This new locality is closest to UCMP V5788, but not close enough to have confidence in the new site as a relocation of the old one.



Figure 8: Field photographs of fossils from the Pilot and Cedar Mountains. A. Antero-posteriorly short vertebra from the Cedar Mountains found in float. Demonstrates characteristic red/purple coloration. B. *In-situ* (IR) and float (FR) ribs from the Cedar Mountains, again demonstrating the characteristic coloration of the area. C. Fossil bones (B) from near the boundary between the middle and upper members of the Luning Formation in the Pilot Mountains. D. Alternate view of the fossils (B) from the middle/upper member boundary of the Luning Formation in the Pilot Mountains. E. Nodular limestone in the Upper Luning, the nodules contained abundant bivalves. F. Phalange from the lower member of the Luning Formation in the Pilot Mountains. G. *In situ* fossil bones from the lower member of the Luning Formation, carrots denote bones. H. *In-situ* ribs from the lower member of the Luning Formation in cross section. Scale Bar: A, B: 10 cm; C, D, F, H: 5 cm; G: 15 cm.

Pilot Mountains:

Vertebrate fossil scouting in the Pilot Mountains located exceptionally abundant fossils of large ichthyosaurs in the lower member of the Luning Formation, and a single vertebrate locality from the boundary between the middle and upper members. Accessing the upper member was difficult but a transect from the top of the lower member through the base of the upper member located 2-3 poorly preserved bone fragments in a wackestone (Fig. 8C-D). The fragments appear to be disarticulated and were not identifiable to a specific taxon. Additionally, forays into the top of the member coming from the north discovered abundant gastropods and bivalves in different horizons (Fig. 8E).

Abundant ichthyosaur fossils were found in all areas where the lower member of the Luning Formation outcrops (Table 1). The fossils are primarily large vertebrae and rib fragments referable to *Shonisaurus*; distal paddle elements and long bones from the limb girdle were also found at some localities. The vertebrae are of substantial size and include some measuring over 30 cm in diameter (Top left corner of Fig. 8G). Despite significant structural deformation, the western face of the Pilot mountains had a particularly high fossil abundance (Fig. 8F-H). Here ichthyosaur fossils are found across all lithologies (i.e., in both bioclastic beds and finer grained interbedded argillite), but the majority of the *in-situ* fossils are in the argillite beds. The material is semi-articulated to disarticulated, and fossils at the surface appear heavily weathered. Fossil preservation does not seem biased towards size, and elements from smaller individuals and the distal portions of the appendicular skeleton have been recovered (Fig. 8F). Invertebrate faunas

are dominated by brachiopods outside of the reef deposits where corals, sponges, and crinoids are observed in higher density.

At the type section for the Luning formation 110 m of the lower member was measured and sampled for microvertebrate fossils (Appendix 2). Samples were taken and processed at 4 m, 32 m, 51 m, 84 m, 92 m, and 108 m along the measured stratigraphic section. The section was chosen based on the structural continuity of the area and the proximity to the contact with the middle member. Ichthyosaur ribs were found *in-situ* at the 20 m mark and in float around the 25 m mark (Appendix 2). Microvertebrate processing yielded negligible results and was deemed not worth pursuing further along the measured section.

Discussion:

Ichthyosaur Abundance in the Luning Formation:

Large ichthyosaur fossils are abundant throughout much of the geographic extent of the Luning Formation in Nevada. Beginning in the Late Carnian at BISP, large *Shonisaurus* become exceptionally abundant (Kelley et al., 2022), and this abundance appears to extend into the Norian in the Pilot Mountains and the Cedar Mountains. The Cedar Mountains in many ways are similar to the Pilot Mountains lithologically and paleontologically, but there are some interesting developments that could warrant further investigation. The sites located in this study are found in rocks of age and lithology that are similar to the ichthyosaur bearing rocks in the Pilot Mountains. However, the possible position for UCMP V6133 is mapped as the upper carbonate member of the Luning Formation which is middle Norian in age (Fig. 4 & 6). Using field notes from the UCMP

archive written by S.D. Webb and J.E. Mawby on a 1961 trip led by Hugh Mottern, V6132 and V6133 can be adjusted to positions that are more consistent with field observations from this study and geologic mapping (Fig. 6). These corrected points still fall above the lower carbonate member and would push the presence of abundant ichthyosaur material to a higher stratigraphic level than what is currently seen in the Pilot Mountains.

The abundance of shastasaurids relative to other taxa is an outlier amongst Late Triassic marine faunas, and yet Nevada seems to preserve this oddity from the late Carnian into the Norian and across a variety of water depths (Martindale et al., 2012; Balini et al., 2015; Kelley et al., 2022; and Fucelli et al., 2023). Based on new fossils preserving cutting teeth, *Shonisaurus* is classified as a raptorial predator with a diet that consisted at least partially of large prey (Kelley et al., 2022). This size class of prey does not appear to be preserved in the Luning formation of Nevada, and Kelley et al. (2022) proposed that *Shonisaurus* must have been a wide-ranging predator that fed outside of the waters preserved in the Luning Formation at BISP. They further propose the Luning at BISP as a breeding ground for *Shonisaurus*. This unique ecological interpretation may extend to the Luning Formation in the Pilot and Cedar Mountains barring future discoveries of more variance in body size or taxa in these two ranges. The Luning Formation sits as a unique part of the range of large shastasaurid ichthyosaurs along the western coast of Pangea that stretched from Sonora, Mexico up into Alaska (Kelley et al., 2023).

The Upper Carbonate Member of the Luning Formation:

The upper carbonate member of the Luning Formation in the Pilot Mountains remains largely unexplored for vertebrates, due to the steepness of the exposures and difficulties in accessing these exposures. The invertebrate fauna shifts from a brachiopod and coral dominated assemblage with prominent reefs in the lower member to a bivalve and gastropod dominated fauna with a distinct lack of reefs (Sandy and Stanley, 1993; Martindale et al., 2012; and Fucelli et al., 2023). Between the deposition of the upper and lower carbonate members of the Luning Formation in the Pilot and Cedar Mountains, a deltaic fan developed and is now preserved as the middle clastic member (Oldow, 1981; Brown, 1986). Large ichthyosaur remains are unlikely to be preserved in deltaic deposits, but the lack of prevalent large ichthyosaur remains in the overlying carbonates raises more questions. The upper member is still interpreted to be a shallow marine ramp deposit, but a change in fauna or depositional environment could factor into a reduced prevalence of large ichthyosaurs.

The Pamlico Formation:

The chronologically equivalent Pamlico Formation in the nearby Garfield Hills differs starkly, with ichthyosaurs and vertebrates of any kind being completely absent. Age constraints on the Pamlico are not well defined. The overlying Gabbs Formation provides a hard upper age limit with biostratigraphic indicators from the Norian, but the lower age limit can only be loosely defined as younger than the Early Triassic based on lithologic comparisons with other volcanogenic units in the region (Oldow, 1978). The invertebrate faunas in the Garfield Hills are poorly preserved, and most of the material is fragmented and not identifiable. The depositional environment in the Pamlico Formation

is interpreted to be shallower than what is seen in the Luning Formation, and as such may have been outside of the preferred habitat for these large marine predators (Oldow, 1978; Martindale et al., 2012; and Balini et al., 2015). Additionally, the Pamlico formation is only seen in the Pamlico-Lodi assemblage which is structurally distinct from the Luning Formation in the Luning-Berlin assemblage (Crafford, 2007). This separate allochthonous assemblage may have been geographically distinct enough from the rocks in the Luning-Berlin assemblage to explain a shift in vertebrate fossil prevalence. These factors along with areas with poor exposure and others with high levels of structural deformation make the Pamlico less ideal for potential ichthyosaur fossils.

III. New York Canyon Ichthyosaur

Objectives and Significance:

The specifics of ichthyosaur ecology and evolution in the later stages of the Triassic are not well understood. This is significant because the two last stages of the Late Triassic, the Norian and Rhaetian, account for over half of Triassic time (35.5 Ma; Cohen et al., 2019). The fossil record of ichthyosaurs and other marine reptiles during these two stages is poor with few localities that are limited to poorly preserved incomplete fossils. Reports of incomplete Norian and Rhaetian ichthyosaur fossils are not especially uncommon and occur globally, but localities with articulated fossils are exceptionally rare. For the entire Norian, there is only one locality worldwide that is known to contain relatively abundant articulated ichthyosaurs, the Pardonet Formation in British Columbia. There are currently no known localities with articulated ichthyosaurs in the Rhaetian, instead bone beds with abundant but disarticulated material that include

ichthyosaur material are the only known fossil localities. This lack of high-quality localities has led to only six named ichthyosaur taxa from the Norian, and none for the Rhaetian, this compared with eight taxa for the Carnian and 23 for the Middle Triassic illustrates the comparatively poor fossil record (Bardet et al., 2014).

In addition to the noted lack of articulated Rhaetian ichthyosaurs, there are no named genera of ichthyosaur that are exclusively and unequivocally from the Rhaetian. The previously mentioned isolated bones and fragmentary skeletons of large to giant ichthyosaurs that occur in several known Rhaetian localities in central and western Europe have all been tentatively assigned an affiliation to the genus *Shonisaurus*. These sites include the famous Rhaetic bonebeds of the U.K. (Lomax et al., 2018) and Germany (Sander et al., 2016), some French localities (Fischer et al., 2014), and a few high elevation localities in the Swiss Alps (Sander et al., 2021; Callaway and Massare 1989). The isolated bone shafts from the U.K. had previously been interpreted as dinosaur leg bones (Redelstorff et al., 2012). The material of giant ichthyosaurs from the Alps was only recently described in detail and consists of fragmentary skeletons and most notably, a very large isolated, incomplete tooth (Sander et al., 2021). In summary, our understanding of the Rhaetian ichthyosaurs is greatly hindered by fragmentary preservation and often uncertain stratigraphic origin.

The scattered remains seen throughout Europe in the Tethys paleo-ocean are notably less common in Panthalassa. The only unequivocal shastasaurid postdating the Carnian *Shonisaurus popularis* in Panthalassa is the Middle Norian *Shonisaurus sikanniensis* (Nicholls and Manabe, 2004). This raises the possibility that shastasaurids went extinct in Panthalassa following the Middle Norian prior to the ETE. However,

scattered remains have been reported from the Late Norian-Rhaetian rocks of Nevada. The partial ichthyosaur remains noted in the literature have primarily come via studies focusing on invertebrates and seemingly failed to garner significant interest for further research. An isolated vertebra was noted in the Norian Nun Mine member of the Gabbs Formation, but was not collected or figured (Laws, 1982). Additional vertebrae and isolated teeth were reported from Ferguson Hill, but again the material seemed to be disarticulated and partial (Taylor et al., 2000; Lucas et al., 2007). Of the material mentioned just a single tooth was figured (Taylor et al. 2000). The tooth is of comparable size to those known from *S. popularis*, but it is partial and missing much of the crown. This study aimed to relocate the sites mentioned in past publications to identify the ichthyosaur remains more precisely. The survey would also aim to find *in-situ* ichthyosaur remains and determine if the material in the region is isolated.

Here we report new *in-situ* and associated vertebrate fossils from the late Rhaetian of the Gabbs Formation at Ferguson Hill. The fossils in association comprise an individual that is comparable in size and shape to *Shonisaurus* and represents the most complete giant ichthyosaur from the Rhaetian. Additionally, the bone-bearing horizon lies less than 2 meters below the negative $\delta^{13}\text{C}_{\text{org}}$ excursion that marks the beginning of the ETE in this section. This specimen indicates that giant ichthyosaurs did not go extinct during the Norian in Panthalassa. Instead, they persisted until the ETE, perishing as a casualty of the mass extinction event.

Materials and Methods:

Geological Setting:

more prevalent near the contact with the overlying Muller Canyon Member. The Gabbs Formation is found in the Gillis Range, Garfield Hills, Paradise Range and Shoshone Mountains, though it is not differentiated from the Jurassic Sunrise Formation in these locations (Muller and Ferguson, 1936). Basin analysis based on the much thicker and more geographically widespread underlying Luning Formation found an original northwest basin-southeast shore orientation for the Luning (Speed, 1978; Reilly et al., 1980; Oldow, 1984). This orientation indicates that the Gabbs Formation also accumulated in the landward portion of a back-arc basin along the western margin of Pangea (Clement and Tackett, 2021).

Ferguson Hill stratigraphy:

Given that this section had been proposed as a potential GSSP for the Triassic-Jurassic boundary, there exists a large number of papers describing the stratigraphy along Ferguson Hill, including detailed stratigraphic sections with lithostratigraphy, paleontology, and geochemistry. The base of the section at Ferguson Hill is composed of the top of the Mount Hyatt Member of the Gabbs Formation (Guex et al., 2004; Lucas et al., 2007; Clement and Tackett, 2021). The top of the Mount Hyatt Member is primarily composed of bioclastic wackestones and siltstones (Lucas et al., 2007). The marker bed AC5, a bioturbated siltstone, is predominately siliciclastic and lies near the base of the section at Ferguson Hill (Guex et al., 2004; Lucas et al., 2007). Overlying the Mount Hyatt Member is the Muller Canyon Member, a primarily siliciclastic siltstone with rare fossils (Laws, 1982; Lucas et al., 2007). Lying 2.1 m above AC5, the marker bed N3 is a dark brown bioturbated siltstone that coincides with a large negative carbon isotope spike

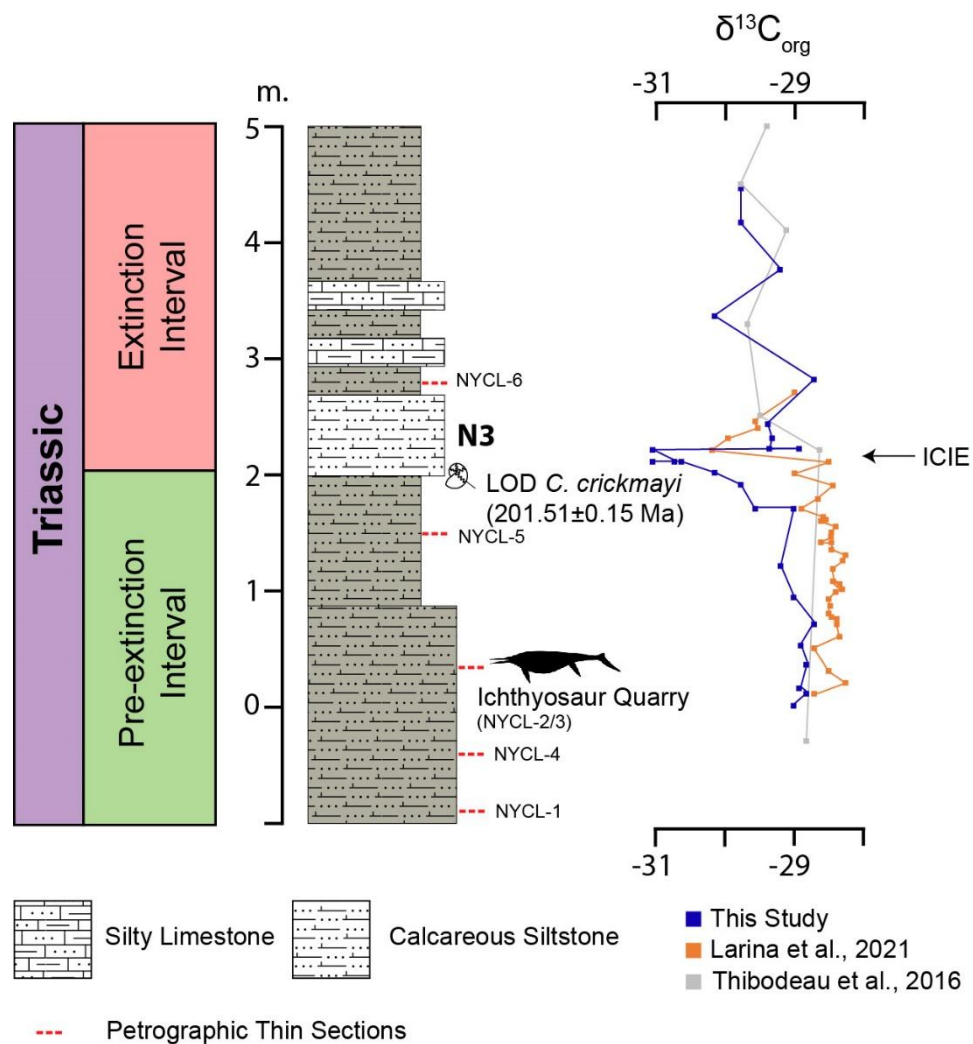


Figure 100: Stratigraphic section from Ferguson Hill, Muller Canyon, Nevada from Larina et al. (2021). The base of the extinction interval is marked by bed N3 in Lucas et al., 2007) and defined by the last occurrence of the *Choristoceras crickmayi* and coincides with the initial carbon isotope excursion (ICIE) (Larina et al., 2021). The data from this study is depicted in blue and the location of the ichthyosaur quarry is marked with an ichthyosaur silhouette. The data from Thibodeau et al. (2016) is depicted in grey, and the data from Larina et al. (2021) is depicted in orange. The last occurrence date for *C. crickmayi* is from Wotzlaw et al. (2014).

and the last occurrence of the ammonite *Choristoceras crickmayi* (Guex et al., 2004; Lucas et al., 2007; Larina et al., 2021). Bed N9, a more resistant carbonate siltstone, contains the first appearance of *Psiloceras spelaë*, and defines the boundary between the Jurassic and Triassic in this section and lies 8 m above bed N3 (Lucas et al., 2007).

The section at Ferguson Hill has been the site of multiple $\delta^{13}\text{C}_{\text{org}}$ studies looking to explore the geochemical signal attributed to the onset of CAMP volcanism and other signals of ecological change (Guex et al., 2004; Ward et al., 2007; Thibodeau 2016; Larine et al., 2021). The exact stratigraphy of the Ferguson Hill section was disputed in two of these studies (Guex et al., 2004; Ward et al., 2007; Guex et al., 2009). Guex et al. (2004) was the first study to run $\delta^{13}\text{C}_{\text{org}}$ on the section, but their findings were challenged by Ward et al. (2007). The subsequent study measured an additional ~8m of section that were not measured in Guex et al. (2004). Guex et al. (2009) challenged the new study, claiming that Ward et al (2007) missed a fault that caused a repeat of stratigraphy near the base of the section. The interpretation of a fault as the cause of the repeat in stratigraphy is challenged by new observations based on excavation revealing more outcrop.

Materials and Methods:

- Field Methods

Excavations were conducted under the guidance of the Natural History Museum of Utah (NHMU) paleontology lab. Overburden removal was done by hand with picks and shovels. Finer tools were employed when the quarry surface approached roughly 30 cm above the bone horizon. Fossils were then systematically located through removal of the final amounts of overburden. The individual elements were then traced until they ended or were truncated by faulting. Jackets were planned based on the ability to trench around groups of fossil elements safely with limited damage to other fossils. Fossils were jacketed using gypsona bandages for smaller fossils and burlap and plaster for larger

jackets. Throughout the excavation process and prior to jacketing, quarry mapping was done using a 1 m x 1 m square subdivided into 10 cm x 10 cm squares and a plumb bob. The 1 m grid was stabilized on poles and leveled using a Brunton Transit compass. The plumb bob was used to locate the fossils' position in the grid so that it could be mapped on the 2D mapping sheets. During the 2022 field season, lidar scanning using an iPhone 12 pro was utilized to supplement the analog quarry mapping.

- Isotope data

Samples were taken for $\delta^{13}\text{C}_{\text{org}}$ geochemistry at variable intervals based on ease of sampling and areas of interest. These samples were powdered and processed for analysis in the mass spectrometer at the UNR Stable Isotope lab. Following initial results, additional samples were taken at a higher resolution around a major negative carbon isotope excursion. The primary aim of the $\delta^{13}\text{C}_{\text{org}}$ sampling was to accurately locate our quarry relative to the published $\delta^{13}\text{C}_{\text{org}}$ data from Ferguson Hill to constrain the age of the site relative to the ETE. These data were collected as part of an undergraduate research project completed by Saige Howard. This project was supervised by myself and my advisor Dr. Paula Noble. Details on the project were presented at the Nevada Undergraduate Research Symposium in Spring, 2022.

- Petrography – thin sections

Samples for petrographic analysis were taken from in and around the quarry site to provide comparative samples for carbonate microfacies analysis, as this type of work was useful in helping to resolve placement in the stratigraphic sequence, based on the work previously conducted at New York Canyon (Lucas et al., 2007; Clement and Tackett 2021). During sample collection, stratigraphic distance from the bone horizon

and stratigraphic up were noted. Following collection, the samples were cut into billets and shipped to Wagner Petrographic where the slides were finished. Imaging and analysis were primarily conducted at the University of Utah's Marine Paleoecology Lab using a Zeiss Axio Imager Polarizing Microscope.

- Fossil Preparation

The bones collected were prepared at the NHMU Fossil Preparation Lab.

Preparation methods include the use of paraloid B-72 solutions to stabilize and connect broken bones, and matrix removal by repeated mechanical preparation with a Paleo Tools Micro Jack air scribe and assorted dental tools. Much of the collected material remains at NHMU for future preparation.

- Histology methods

Samples of ribs were cut and prepared for histological analysis at the NHMU, as this method can be diagnostic for certain taxonomic groups of ichthyosaurs (Perillo, 2022). Sample preparation roughly followed the methods outlined in *Bone Histology of Fossil Tetrapods* by Padian and Lamm (2013). For curatorial purposes, samples selected for destructive analysis were first molded and cast to make a replica of the original fossil. Following successful molding and casting, the fossils were then embedded in resin to stabilize the sample during cutting and grinding. A wafer was then cut from the embedded fossil and attached to a frosted glass slide. The now mounted sample then underwent further thinning with a rock saw before beginning the grinding process. Grinding of mounted samples was done by hand using a range of silicon carbide powder grits on glass plates. Sample thickness was gauged throughout the process based on translucence and measured periodically using a set of digital calipers. Final thickness was

approximately 100 μm . Finished slides were imaged and analyzed using a Zeiss Axio Imager Polarizing Microscope at the Marine Paleocology Lab at University of Utah.

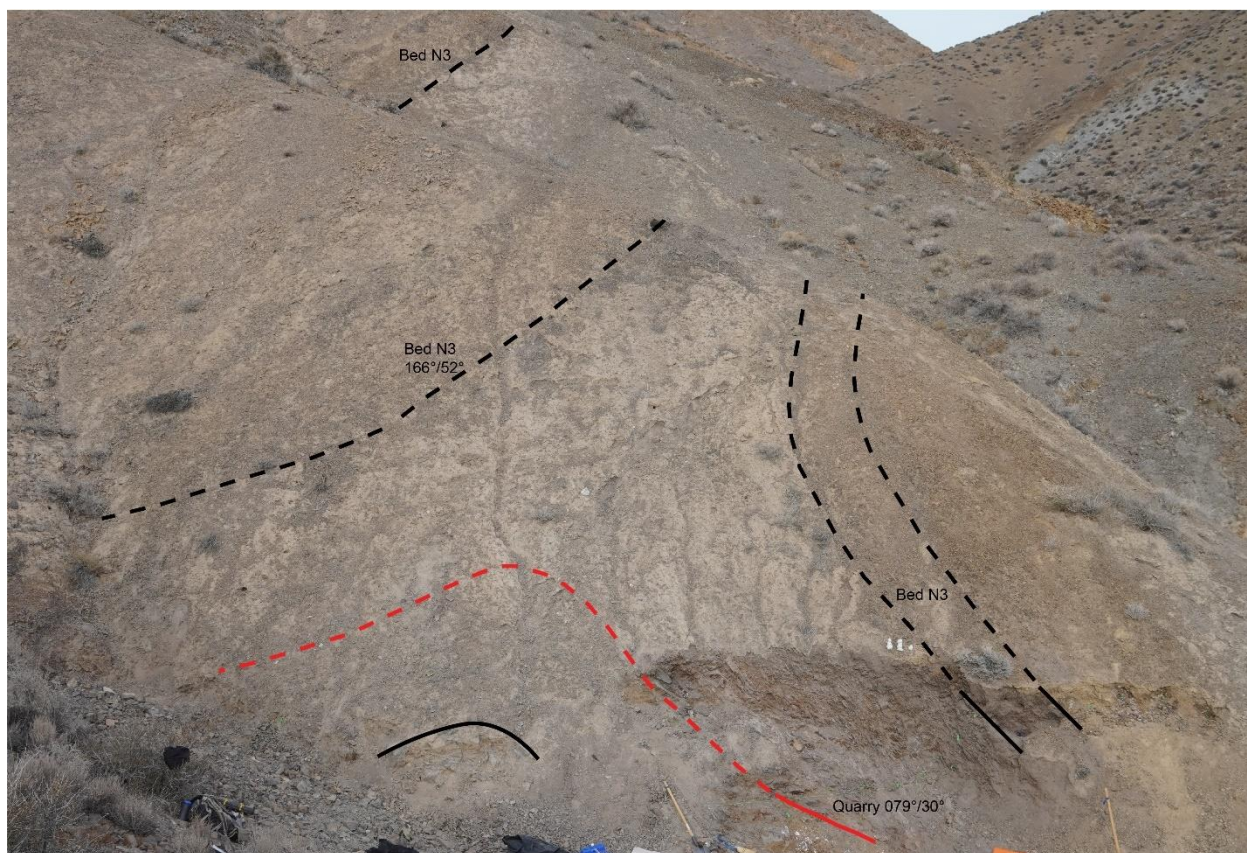


Figure 11: Perspective view of the quarry and surrounding southern slope of Ferguson Hill at Muller Canyon. The solid black curve at the bottom of the photo traces the bedding plane of the proposed fold hinge. The bone horizon is traced in red and projected beyond the quarry based on the structure of the underlying bed.

Results:

Field observations of quarry stratigraphy and structural geology:

Initial observations placed the stratigraphic location of the quarry below bed N3 following the conventions from Lucas et al. (2007) (Tackett, personal communication). The excavation of the quarry site revealed more of the bedding and it was observed to dip to the southeast, contrasting with an observed west-northwestern dip for beds above the quarry site. Additionally, a nearby fold hinge was identified, and the dark N3 marker bed

appeared to be repeated on both sides of the hinge (Fig. 11). A large normal fault to the south of the quarry projects down the drainage the quarry lies in. This fault is accompanied by a series of smaller offsets present in the quarry itself, changing the orientation of the beds slightly nearest the slope's surface.

Thin section analysis:

Petrographic analysis found that the thin sections from around the quarry are primarily silty carbonate and calcareous siltstone beds with varying carbonate content (Fig. 12). Fossil bioclasts are common at the base of the section but become sparse to absent above the bone horizon. Additionally, silica content in the rock increases moving up section. The samples generally fit the expected facies described in Clement and Tackett (2021), grading from the silty lime mudstone to a carbonate siltstone. However, the base of the bone horizon can best be described as a skeletal packstone most similar to the hashy skeletal packstone facies (HSP) from Clement and Tackett (2021). Fossil bioclasts observed in thin section include bivalves, brachiopods, echinoderms and sponges.

Invertebrate collections:

Ammonites are sparse but present in the uppermost part of the Mount Hyatt Member where the quarry is located. Ammonites found during excavation were all assigned to either the *Choristoceras* or *Arcestes* genera upon collection. Ammonites of the *Arcestes* genus were unable to be identified to the species level due to poor preservation. Ammonites of the *Choristoceras* genus were identifiable to the species level, and

identifications were made using the species descriptions from Taylor et al. (2000, 2021).

A single *C. crickmayi* was found on Ferguson Hill north of the quarry. This contrasts with the quarry where all *Choristoceras* ammonites were identified as *C. shoshonensis*.

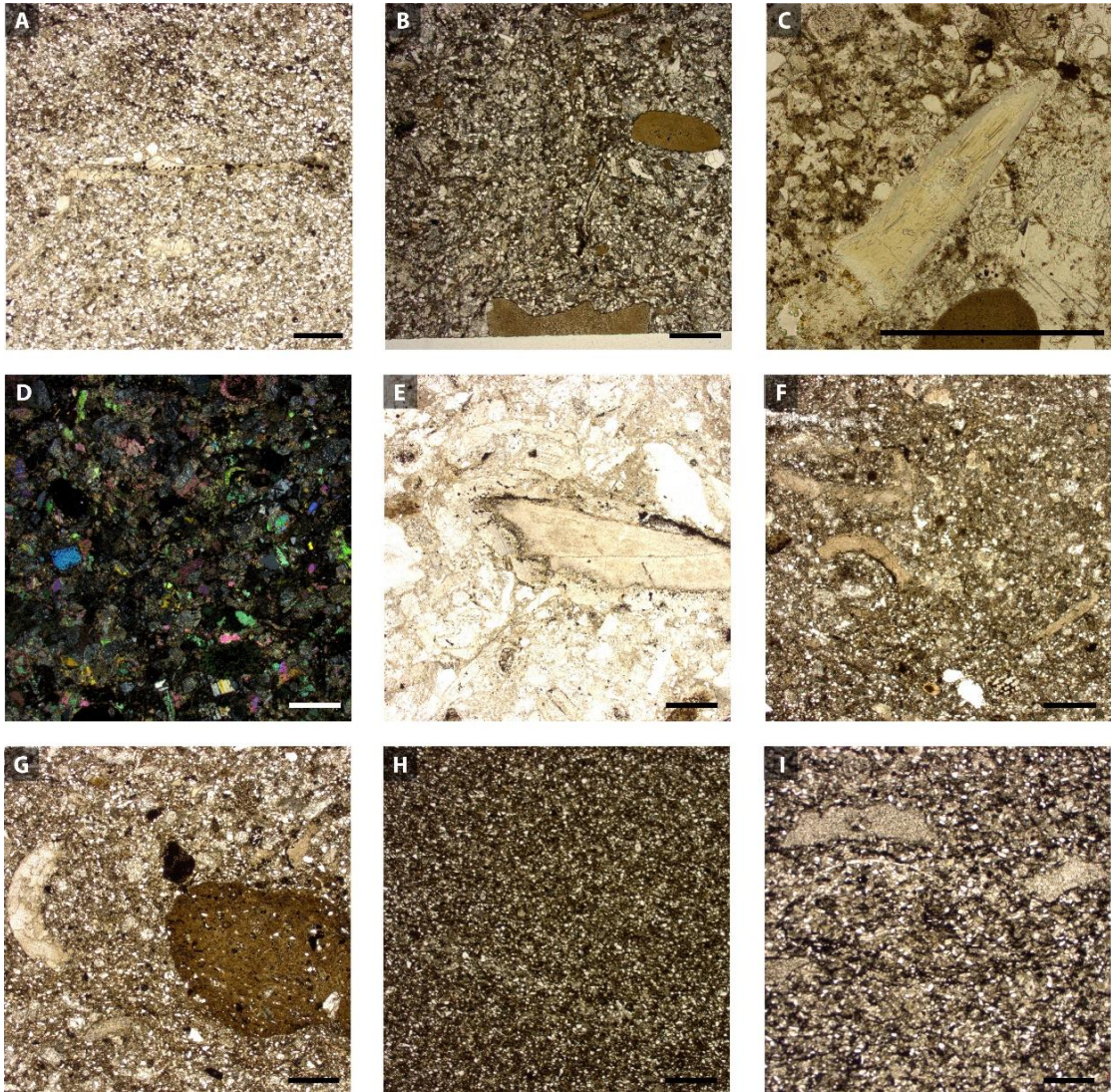


Figure 12: Thin sections of quarry rocks. A) NYCL-1, wackestone with bioclasts. B) NYCL-4, bone and intraclast in wackestone. C) NYCL-4, tooth and intraclast. D) NYCL-2, packstone with echinoderm spine in XPL. E) NYCL-2, packstone with belemnite. F) NYCL-3, bioclasts and silt. G) NYCL-3, bioclasts, intraclast, and hematite. H) NYCL-5, siltstone with characteristic lack of bioclasts. I) NYCL-6, silt and mud sparse but present bioclasts.

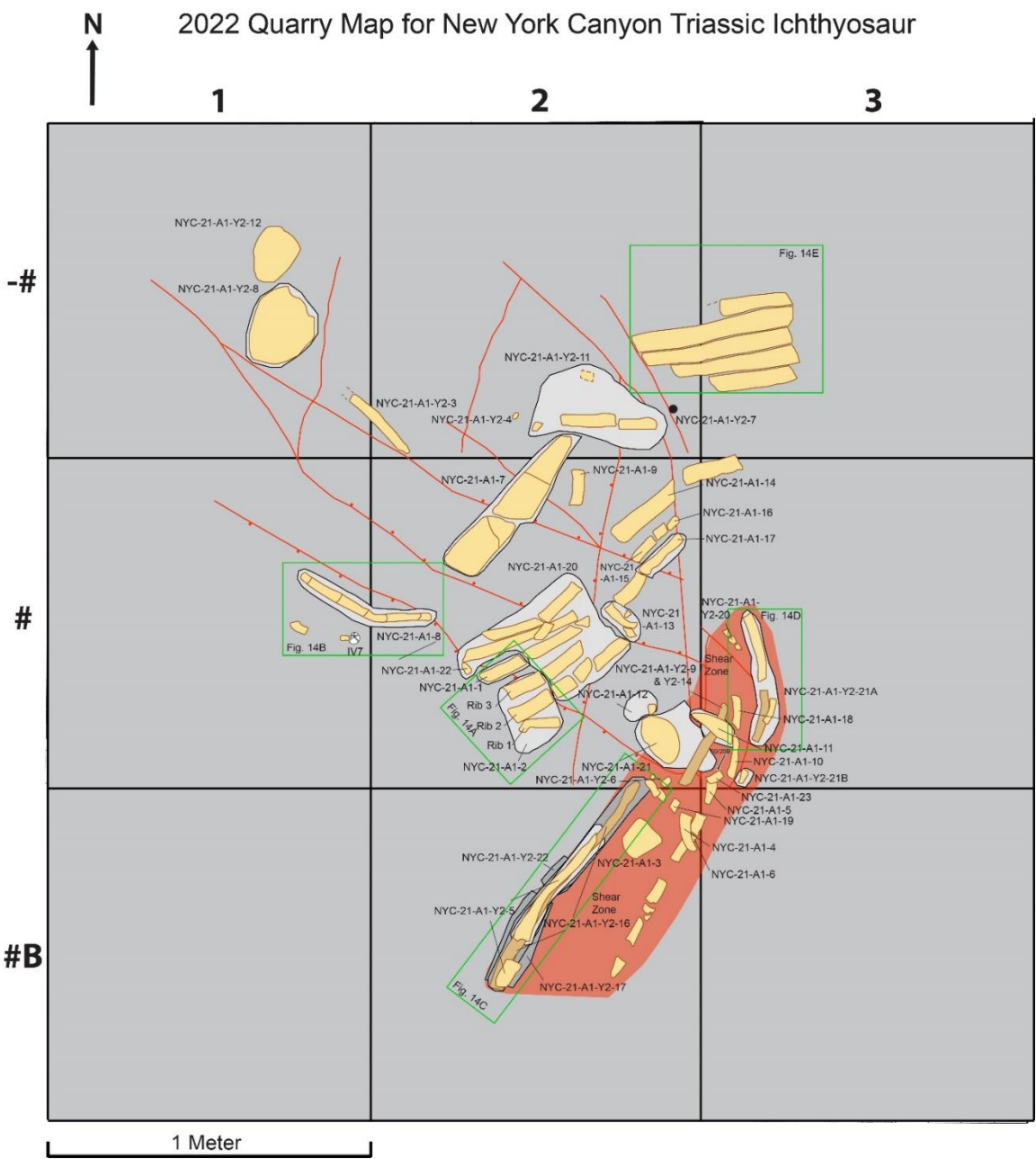


Figure 11: Labeled map of the NYC-21-A1 ichthyosaur quarry as of Fall 2022. The quarry is interpreted to be the semi-articulated remains of a single individual, highly displaced by post-depositional tectonic activity. Locations for Fig. 14 photographs are marked in green rectangles. Tan polygons: fossil bones; Grey polygons: Collected Jackets; Red polygon: region of high deformation (referred to herein as the shear zone); Red lines: small faults.



Figure 12: Field photographs of the NYC-21-A1 ichthyosaur quarry, carrots denote fossil bones. A. Excavation progress from the summer of 2021, 4 partial ribs going into the hillslope. B. Excavation progress from the Fall of 2021. C. A partial rib in the heavily deformed zone, additional ribs would be found underneath this rib. D. Another rib from the deformed zone demonstrating the curve the ribs follow in this area. E. 4 articulated ribs that appear to be diving down as they cross the extension of the deformed zone. Additional partial ribs at the top of the photograph cross the articulated ribs at oblique angles. Locations correspond to Figure 10. Scale bar: 10 cm.

Carbon isotope data:

$\delta^{13}\text{C}_{\text{org}}$ isotope data were collected along a 5-meter section spanning from roughly 50 cm below the quarry through bed N3 (Table 2) (Fig. 10). A baseline of approximately -29‰ vs. VPDB was observed below a -1.7‰ excursion that occurs at the base of bed N3, 2 meters above the base of the 5-meter section and just 1.7 meters above the bone horizon.

Vertebrate collections:

The initial find consisted of 6 rib segments in a bioclastic packstone, 4 of these rib segments were removed in 2 jackets (Fig. 12-13). The next excavation expanded the quarry significantly and exposed more of the 6 previously noted ribs along with more ribs and the 2 centra. The following field season focused on excavating the currently established quarry and discovered a set of 5 articulated ribs (Fig. 14E). The current extent of site NYC-21-A1 consists of at least 17 partial ribs, 2 centra, and an assortment of unidentified bone fragments (Table 3). The material is semi-articulated and represents a portion of the associated postcranial skeleton of a giant ichthyosaur (Fig. 13-14). Two isolated bones were collected from near the quarry, a single small pistosaur centrum and a small rib fragment of indeterminate reptilian affinity. An additional block containing vertebrae of pistosauroid affinity similar in size to the isolated centrum was collected from stratigraphically lower in the early Rhaetian of the Mount Hyatt member.

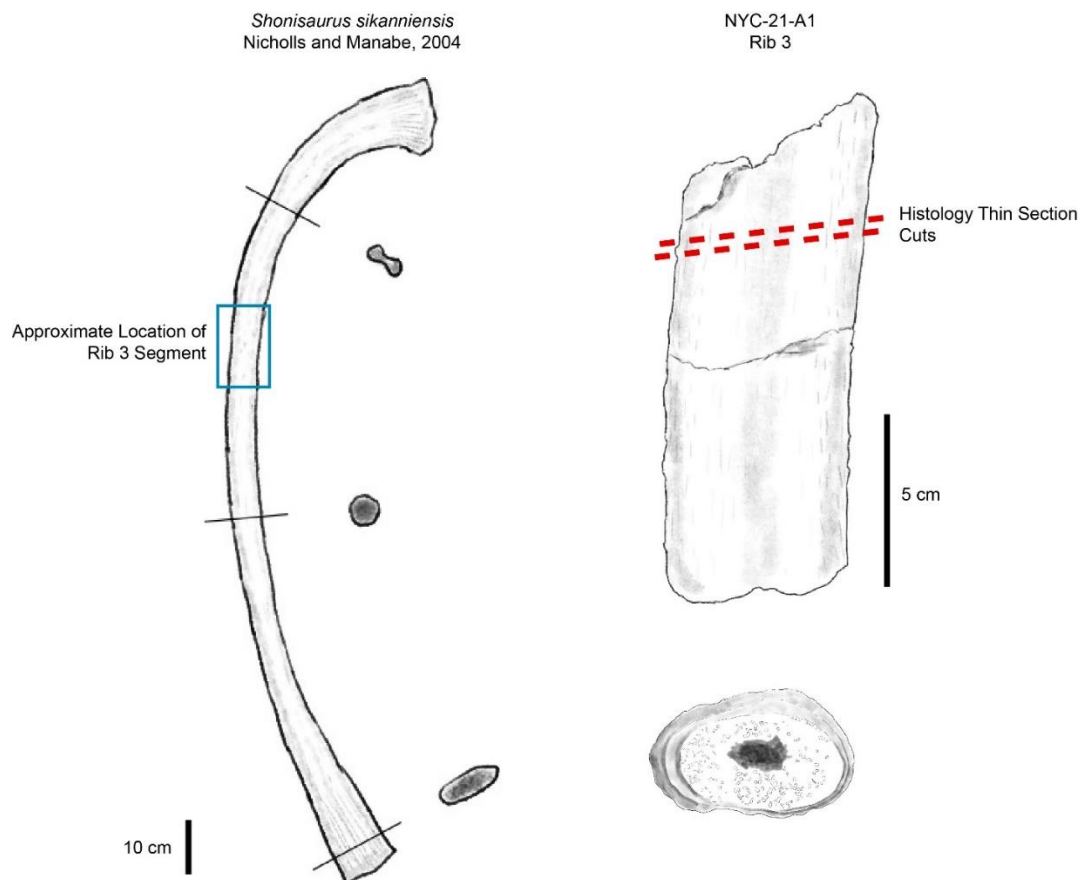


Figure 13: Schematic showing approximate location of rib 3 segment along whole rib and histology thin section cuts on rib 3. At this portion of the rib the cross-section is transitioning from the double grooved figure-eight shape seen at the proximal end to the more circular shape seen around the midline. Whole rib sketch based on Figure 9, Nicholls and Manabe, 2004.

Histology:

Rib 3 from jacket NYC-21-A1-2 was selected for thin sectioning due to its lack of fractures and position at the edge of the hillslope that allowed for sectioning on a section of the rib that is guaranteed to not connect to additional rib fragments (Fig. 13&15). In both plane and cross polarized light there are clear rhythmic growth marks visible in the cortical bone (Fig. 16A & 16C). There does not appear to be any difference in density between the growth marks, but there is a marked difference in color. The primary cortical tissue is built up via a woven-parallel complex, where the woven component is made up of interwoven structural fibers tissue, while the parallel component is composed of

lamellar bone along the primary osteons. The interwoven structural fibers tissue is most easily recognized under cross polarized light where it is recognized as a birefringent network of rectangular and polygonal shaped units of varied sizes (Fig. 16D) (Perillo, 2022). The center of the rib is highly cancellous contrasting starkly with the much denser cortical bone. The rib is characterized by longitudinal vascularization that varies in shape from modestly circular to quite abstract.

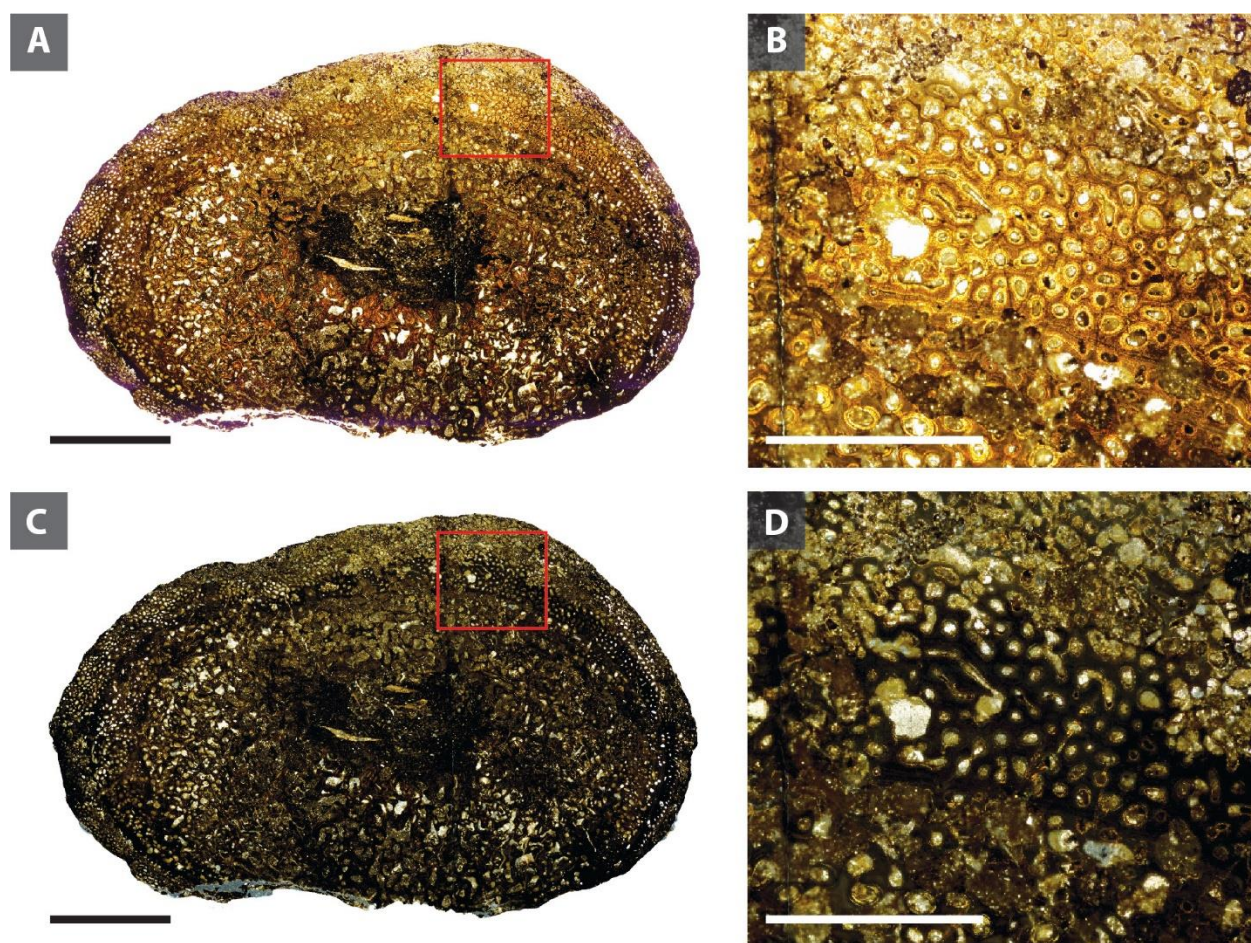


Figure 14: Thin section photomicrographs of rib 3 from NYC-21-A1-2. A. Whole slide scan in plane polarized light. B. Close up on red square from A. C. Whole slide scan in cross polarized light. D. Close up on red square from C, note the small birefringent polygons seen in the cortical bone.

Discussion:

Geological interpretations:

It is important to determine the age of the ichthyosaur with a high level of precision, due to the site's location close to the Triassic/Jurassic boundary, and the importance of the end-Triassic extinction in the evolutionary history of ichthyosaurs. The stratigraphy of New York Canyon is quite well studied and provides excellent age control when compared to other Rhaetian ichthyosaur localities. Ammonites are one of the best studied and easiest to find biostratigraphic groups in the New York Canyon area, providing an even more precise control over the Late Rhaetian than similar biostratigraphic zones in the Tethys (Taylor et al., 2021). Ammonites become less common and more poorly preserved in the latest Rhaetian of New York Canyon (Clement and Tackett, 2021), but multiple specimens were successfully collected during quarry excavation. The ammonite biozones for the late Rhaetian in North America are the *Choristoceras rhaeticum* zone and the overlying *C. crickmayi* zone, which split the *Choristoceras marshi* zone used in the Tethys (Fig. 17). Neither of these ammonites were collected from the quarry, but multiple specimens of *C. shoshonensis* were found in association with the ichthyosaur alongside less stratigraphically useful ammonites from the *Arcestes* genus. *C. shoshonensis* is found in association with the *C. crickmayi*, providing a confident placement of the ichthyosaur inside of the latest Triassic *C. crickmayi* biozone (Taylor et al., 2021; Taylor et al., 1983). The ammonite biostratigraphy is further supported by the presence of burrowing bivalves *Nuculoma*. The *Nuculoma* assemblage (Laws, 1982), is characteristic of the latest Triassic in the New York Canyon area (Clement and Tackett, 2021; Tackett and Bottjer, 2016).

Ammonoid Zonation		
North America		Tethys
Rhaetian	<i>Choristoceras crickmayi</i> Zone	<i>Choristoceras marshi</i> Zone
	<i>Choristoceras rhaeticum</i> Zone	
	<i>Cycloceltites tozeri</i> horizon	<i>Vandaites stuerzenbaumi</i> Zone
	<i>Vandaites newyorkensis</i> Zone	
	<i>Paracochloceras amoenum</i> Zone	<i>Sagenites minaensis</i> Subzone
<i>Sagenites striata</i> Subzone		
Norian	<i>Gnomohalorites cordilleranus</i> Zone	<i>Sagenites quinquepunctatum</i> Zone

Figure 15: Correlation of ammonoid and zonations between North America and Tethyan Europe. Modified from Taylor et al, 2021.

The Gabbs formation in the proximity of the ichthyosaur quarry was interpreted to be a relatively shallow environment transitioning from a mid-ramp to inner ramp setting. based on the microfacies observed in thin section. The skeletal packstone seen at the base of the bone horizon seems to fit the interpretation of the HSP facies from Clement and Tackett (2021), representing the deposition of bioclastic shoals on the mid to inner ramp transition. This facies represents a high energy setting due to the abundance of fragmentary skeletal grains and fine sand matrix (Fig. 12). The silty lime mudstone observed in most of the quarry is interpreted to represent deposition in a lower energy inner ramp transition setting. The carbonate mudstones with abundant and visible

siliciclastic very fine sand to silt grains indicate that this facies was likely relatively close to the terrigenous source. The noted decrease in overall grain size may be due to a slight increase in water depth landward of the discontinuous bioclastic shoal interpreted from the packstone sample. The calcareous siltstone observed at the top of the quarry is interpreted to represent a deposition on a tidal flat in the distal inner ramp. The high percentage of fine quartz grains and lack of fossils that would be expected of deeper water deposition support this interpretation.

The presence of geological structures in the area, including a normal fault in the drainage, and the presence of the anticline in the quarry, prevented a more continuous stratigraphic transect from being collected for microfacies and $\delta^{13}\text{C}_{\text{org}}$ analysis. However, the data collected have been sufficient to determine the stratigraphic position of the quarry and the ichthyosaur beds as 1.7 meters below the end-Triassic Extinction, and 8 meters below the Triassic-Jurassic boundary, as described in previous work. Previous work on the $\delta^{13}\text{C}_{\text{org}}$ near the quarry site had interpreted an additional normal fault to the immediate south of the quarry that in turn caused a repetition in the $\delta^{13}\text{C}_{\text{org}}$ data and stratigraphy (Ward et al., 2007; Guex et al., 2009). More recent $\delta^{13}\text{C}_{\text{org}}$ transects on nearby hills have avoided the area around the quarry due to the increased structural complication, however Larina et al. (2021), used the interpretation from Guex et al. (2009) to correct the data from Ward et al. (2007) and found that the different data collections seemed to agree when this fault was accounted for (Fig. 10). As we began our work at the quarry site, it became clear that the observed change in dip direction near the quarry and the nearby fold hinge challenged the interpretation of a fault in the area, and instead led us to interpret a fold in the area (Fig 11).

Proximity to the ETE

We are interpreting the observed -1.7‰ $\delta^{13}\text{C}_{\text{org}}$ excursion 1.7 meters above the bone horizon as the initial carbon isotope excursion (ICIE). This excursion matches the amplitude of the ICIE noted in previous studies and is present at the base of bed N3, where other studies in this area located the ICIE in the past (Fig. 12). The data above and below the excursion also closely match data from previous studies taken from sections north of the quarry on Ferguson Hill, away from the structural complication. This provides support for our interpretation of a small fold and our choice to sample in the opposite direction of Ward et al., 2007 and other previous studies that sampled farther away from the structural complications.

The proximity of the bone horizon to the ICIE raises the question: is this the youngest shastasaurid ichthyosaur? There are no known identifiably shastasaurid ichthyosaurs from the Jurassic. A single specimen from Wales was initially reported as Jurassic in age, but it was collected loose on the beach with poor stratigraphic constraints (Martin et al., 2014; Lomax et al., 2018). The German, Swiss, and French localities are all better constrained than the Welsh locality, but the stratigraphic controls are less precise than those at New York Canyon. The best biostratigraphic control is the early-middle Rhaetian bivalve *Rhaetavicula contorta* (Sander et al., 2022; Fischer et al., 2014). This leaves the ichthyosaurs from the U.K. as the primary competition for the title of youngest shastasaurid. The Lilstock specimen is located 0.8 m below the contact between the Westbury Mudstone Formation and the Cotham Formation (Lomax et al., 2018). A negative carbon isotope excursion has been recognized ~ 1.1 m above the base of the Cotham Formation (Percival et al., 2017), placing the Lilstock ichthyosaur just 1.9 m

below the onset of the extinction. However, Fox et al. (2020) argued that the observed carbon isotope excursion seen here is due to regional environmental change and not equivalent to the globally recognized ICIE. The onset of the ETE at these sites is now recognized to be ~3.6 m above the base of the Cotham Member, which is ~4.4 m above the Lilstock ichthyosaur horizon.

NYC-21-A1 lies just 1.7 m below the ICIE at New York Canyon, but stratigraphic distance is not a proxy for time due to differing sediment deposition rates. Two lines of evidence show that the sedimentation rate at New York Canyon is faster than those at the U.K. site suggesting the New York Canyon Ichthyosaur is stratigraphically closer to the ICIE. First, geochemical data shows a greater stratigraphic distance between the ICIE and the beginning of the Jurassic at New York Canyon (Percival et al., 2017, Fig. 3). The St Audries/Lilstock sections don't have ammonoid biostratigraphic control for the Triassic part of the section, but the zones for the Jurassic can be used to provide further control over sedimentation rate throughout the section. At Lilstock/St. Audries, the boundary between the *tilmanni* and *planorbis* zones is ~5m above the base of the ETE, whereas at New York Canyon it is ~13 m above the base of the ETE (Percival et al., 2017). This again supports a higher sedimentation rate at NYC, and thus the 1.7 m distance at NYC is likely equal to less time than the equivalent thickness at St Audries/Lilstock in addition to the Lilstock ichthyosaur being stratigraphically farther from the ETE.

Taxonomic interpretations:

This specimen is an important addition to understanding the ichthyosaurs of the global Rhaetian as the most complete associated shastasaurid skeleton from the Rhaetian.

The existing Norian shastasaurid taxonomy only includes three named valid species: *S. popularis*, *S. sikanniensis*, and *Himalayasaurus tibetensis*. All three of these named species are significantly older than NYC-21-A1. Determining if the new specimen can be referred to one of the existing taxa is an important first step. However, it is difficult to accomplish this due to the limited nature of the find and the limited variability in rib morphology. Grooving on the anterior and posterior sides of the rib has been noted as a variable feature in shastasaurids (Sander et al. 2022). Both *S. sikanniensis* and *S. popularis* share the antero-posteriorly grooved proximal rib ends seen in NYC-21-A1, however it is not consistent throughout the entirety of the animal (Nicholls and Manabe, 2004; Camp, 1980 contra text). Of the three European localities that preserve ribs, two of the sites (Bonenburg and Cuers) preserve the figure-8 cross section seen in the proximal portion of *S. sikanniensis* and *S. popularis* (Perillo, 2022; Fischer et al., 2014). The ribs from the Swiss Alps differ from these examples, showing only an anterior groove (Sander et al., 2022). Sander et al. (2022) notes this difference in morphology when describing the material from the Swiss Alps, but the variability noted in the Nicholls and Manabe (2004) calls the importance of this into question. The histology of the sectioned rib shares many similarities with the ribs sectioned by Perillo (2022). Possibly most diagnostic is the presence of the interwoven structural fibers that is seen in the cortical bone. This feature has not been noted in many taxa outside of large shastasaurid ichthyosaurs and larger nothosaurs (Redelstorff et al., 2012; Klein et al., 2019; Perillo, 2022).

Size proxies for ichthyosaurs based on mostly incomplete skeletons and isolated bones are rough approximations, but relative size comparisons for individual bones can provide some insight into relative body size. The most complete shastasaurid ichthyosaur

is the 21-m *Shonisaurus sikanniensis* holotype. The skeletons from BISP are the next most complete. Camp (1980) estimates the length of specimen BISP A-5 (with composited tail from BISP C) to have been 15.7 m. Kosch, (1990) and McGowan and Motani, (1999) agree and give estimates of 15 m. Body mass estimates came along more recently with Gutarra et al., (2019). Digital volume models resulted in a mass of 29.7 metric tons for a *Shonisaurus popularis* of 15 m length. General size proxies are difficult to find for these giant ichthyosaurs because of our incomplete knowledge of their anatomy. Vertebral dimensions appear most suitable, but there is the caveat that vertebral numbers are high and variable in *Shonisaurus* and *Shastasaurus*. In fact, *Shastasaurus liangae* has over 80 presacral vertebrae and over 110 caudal vertebrae, the highest number for any ichthyosaur (Sander et al., 2011). Due to these challenges, exact size estimates for anything but a nearly complete ichthyosaur are unfortunately limited to rough approximations and relative size comparisons between similar material.

The largest rib collected from NYC-21-A1 measured 73.1 mm in diameter at the proximal shaft of the rib (Table 4). This measurement is larger than measurements along similar rib positions for both *S. sikanniensis* and *S. popularis* (Nicholls and Manabe, 2004, from figures; personal observations). Using rib size as a rough proxy would place this ichthyosaur at greater than the 21 m length estimated for the *S. sikanniensis* holotype. Nicholls and Manabe (2004) did report individuals of even greater size in the Pardonet Formation. Fossils of these individuals were not collected or figured, but diameters of some ribs found in the Pardonet Formation are comparable to and even exceed those from NYC-21-A1 (Sander, personal communications). As such, the new specimen may not be

the largest ichthyosaur to ever live, but it is of truly exceptional size comparable to the largest known ichthyosaurs from the late Triassic.

Systematic Paleontology:

Repository- all materials have been accessioned in the collections of the Utah Museum of Natural History and were collected under permits (N-97238 and N-97239) to Dr. Noble. Detailed information, including preparation status and geographic coordinates may be retrieved through queries to the museum at registrar@nhmu.utah.edu.

AMNIOTA Heckel, 1866

ICHTHYOSAURIA Blainville, 1835

MERRIAMOSAURIA Motani, 1999

SHASTASAURIDAE Merriam, 1902 sensu Ji et al., 2016

Definition – The last common ancestor of *Shastasaurus* and *Besanosaurus*, and all its descendants (from Ji et al., 2016).

Aff. Shastasauridae

Referred Material – Specimen NYC-21-A1, associated partial skeleton (Fig. 13-14) consisting of 2 large partial centra, at least 17 incomplete ribs, and some unidentified bone fragments (Appendix 1). The material is variably tectonically deformed.

Horizon and Locality – Upper Rhaetian Mount Hyatt Member, Gabbs Formation. South side of Ferguson Hill, Gabbs Valley Range, Nevada, United States (coordinates 38° 29' 9.78" N, 118° 5' 0.95" W).

Remarks – Due to the partial nature of the skeleton, the ongoing excavation, and the unprepped state of much of the excavated material, a differential diagnosis is still underway as of July 2023, and not currently available for assigning this material to a taxon beyond the family level. As such, only an affinity to the family Shastasauridae has been assigned, but more specific taxonomic classification may be possible following further excavation and preparation of the material. Descriptions are limited to the prepped material.

Affinities – The partial ribs and centra of NYC-21-A1 differ in their large size from all ichthyosaurs outside of the family Shastasauridae. Among these giant ichthyosaurs, the ribs are still of notable size (Table 4). Some form of antero-posterior compression in the proximal end of the rib is seen throughout the known members of Shastasauridae. With NYC-21-A1, we see variability in the presentation of this compression. The two largest species in Shastasauridae are noted to have grooves along the anterior and posterior sides of the proximal end of the ribs (Nicholls and Manabe, 2004; Camp, 1980). The grooves are not seen throughout the entirety of the spinal column, but the presence of these grooves in some of the ribs from NYC-21-A1 supports a diagnosis as a large shastasaurid.

Description – Specimen NYC-21-A1 represents an associated partial skeleton, although the completeness of the skeleton is currently unknown. At present only a portion of the skeleton is excavated. The known skeleton consists of 2 partial centra, and 17 incomplete dorsal ribs. The specimen has been distorted by thrusting in the Mesozoic and Basin and Range tectonics in the Cenozoic. The specimen is within a few meters of a prominent normal fault and the hinge of an observed fold structure. A prominent zone of

deformation has heavily distorted at least 4 ribs from the site. Ribs outside of this shear zone are considerably less deformed, and thin sectioning has revealed a seemingly intact trabecular architecture.

Vertebral Centrum – The partial centrum NYC-21-A1-3 preserves just less than half of the centrum. The centrum was located in the shear zone and is modestly deformed. The centrum is amphicoelous and would have had a diameter of roughly 20 cm if it was complete. A feature along the side of the centrum appears to be one of the parapophyses. The other partial centrum NYC-21-A1-21 is currently unprepared.

Ribs – Nine of the seventeen currently excavated ribs are preserved in two semi-articulated clusters. An additional four ribs are stacked vertically in the shear zone, in this zone much of the displacement can be attributed to post-depositional tectonic activity. The tectonic displacement and incompleteness of the individual ribs has currently made it difficult to determine orientation of the skeleton and the exact position of the ribs. Based on size, grooving, and the antero-posterior compression of the ribs it can be determined that all of the currently prepared material is of the proximal portion of the rib shaft. The ribs are on average 5.2 cm in diameter, though the largest example is 7.3 cm at its widest point. Grooving along the anterior and posterior sides, forming a figure 8 cross-section, is present on 3 of the prepared samples. Ribs without grooving on both sides, generally still present with a groove along one side of the rib, without further context it is difficult to determine whether this is the anterior or posterior side of the rib.

SAUROPTERYGIA Owen, 1860

PISTOSAURIA Baur, 1887

Pistosauria, indet. A.

Referred Material – Specimen NYC-21-A1-24, single isolated vertebra found in float.

Horizon and Locality – Upper Rhaetian to Lower Hettangian Muller Canyon Member, Gabbs Formation. South side of Ferguson Hill, Gabbs Valley Range, Nevada, United States (coordinates 38° 29' 9.78" N, 118° 5' 0.95" W).

Description – The faces of the centrum are considerably less amphicoelous than would be expected in an ichthyosaur or fish. The dense layer of bone along the faces of the centrum are characteristic of those seen in members of pistosauria, including the plesiosaurs. Wintrich et al. (2017) note that cervical vertebra in plesiosaurs contain two paired foramina along the ventral side of the centrum. Distortion of the vertebra and the need for additional mechanical prep have prevented a firm diagnosis on the presence or absence of these foramina in this specimen.

Remarks – The single isolated vertebra NYC-21-A1-24 was found in the float near the talus pile of NYC-21-A1. The vertebra is quite weathered and was likely on or near the surface for some time. The centrum is gently amphicoelous on the anterior and posterior ends and quite small measuring 2 cm in diameter. The centrum is relatively short in the anteroposterior dimension and tall dorsoventrally. Parapophyses are preserved and sit low on the lateral sides of the centrum. The position of the parapophyses and the dorsoventrally tall, anteroposteriorly short dimensions of the vertebra are most similar to those seen in the last few cervical vertebra of pistosaurs. A portion of the neural arch is attached to the centrum with a hard rind of matrix. Micro-CT

scans revealed a dense layer of cortical bone along both faces of the centrum and a v-shaped pattern of dense bone near the neural canal.

Pistosauria indet. B.

Referred Material – Specimen LST-18-1, 3 associated caudal vertebrae in a single block collected from float.

Horizon and Locality – Rhaetian Mount Hyatt Member, Gabbs Formation. New York Canyon, Gabbs Valley Range, Nevada, United States (coordinates 38° 29' 46.32" N, 118° 5' 1.79" W).

Description – The faces of the centrum are considerably less amphicoelous than would be expected in an ichthyosaur or fish. The dense layer of bone along the faces of the centrum are characteristic of those seen in members of pistosauria, including the plesiosaurs.

Remarks – The block of vertebrae appeared to contain portions of at least three vertebrae, and the cross-section of two of these vertebrae was clearly visible. The centra appear gently amphicoelous with a dense layer of bone along the anterior and posterior faces. Micro-CT scanning provided a more robust view of the vertebrae in the block. The centra of these vertebrae are short along the antero-posterior dimension, but not as dorsoventrally tall as NYC-21-A1-24. The neural arch is taller than the centrum at its peak and does not preserve any diapophyses. Instead, we see small ribs attached to the centrum. The attached ribs are short and extend horizontally from the centrum in a manner that resembles what is expected of caudal ribs.

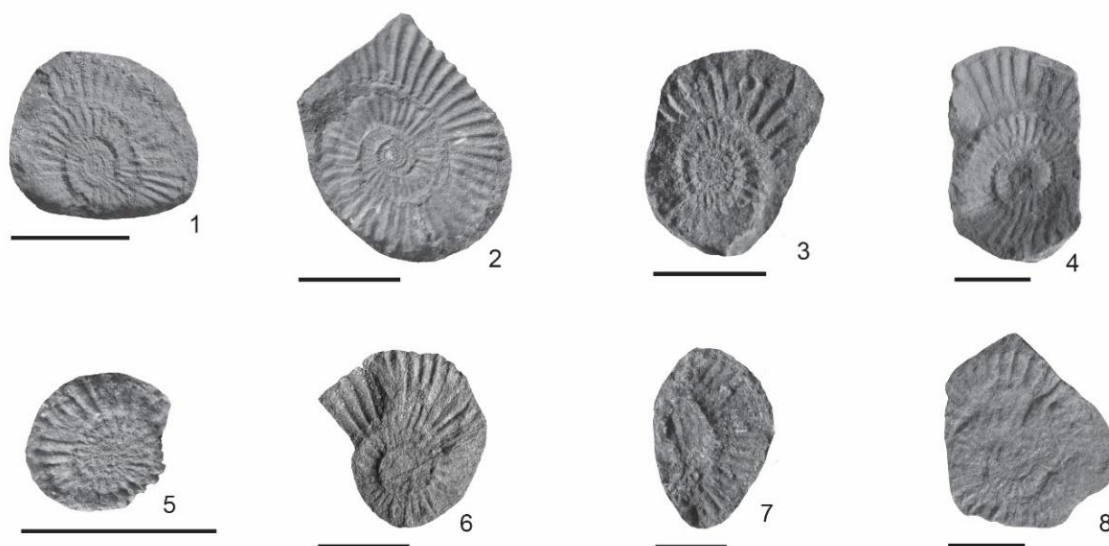


Figure 16: Ammonites from the quarry and Ferguson Hill. *Choristoceras shoshonensis* Taylor & Guex, 2002, 1; 2; 3; 4; 5; *Choristoceras crickmayi*, Tozer, 1979, 6, located outside of the quarry; *Choristoceras* indt., , 7; 8. Scale bar: 1 cm.

CERATITIDA Hyatt, 1884

CHORISTOCERATIDAE Hyatt, 1900

CHORISTOCERAS Hauer, 1865

Choristoceras shoshonensis Taylor and Guex, 2002

Figure 18.1-5

Referred Material – 5 specimens total from the top of the Mount Hyatt Member.

Specimens are located above and below the bone horizon.

Remarks –The identity of these specimens is discernable due to the characteristic serpentine coiling of the whorl and the low whorl expansion rate. The ribbing is also diagnostic when compared to other members of the same genus, appearing more falcooid and varyingly rursiradiate. All examples of *Choristoceras shoshonensis* in the

ichthyosaur quarry present as crushed molds with varying levels of preservation. The specimens occur alongside *Nuculoma* bivalves and *Arcestes nevadanus* in the silty skeletal packstone that defines the bone bearing horizon. They appear to increase in abundance in the silty units overlying the bone horizon.

Choristoceras crikmayi Tozer 1979

Figure 18.6

Referred Material – 1 specimen collected from the base of the Muller Canyon Member outside of the ichthyosaur quarry on Ferguson Hill.

Remarks – The lone specimen is preserved as a compressed mold in a carbonate siltstone. It exhibits a higher whorl expansion rate than *C. shoshonensis* and lacks serpenticone inner coils. It can be distinguished from *C. marshi* based on its radial ribbing as opposed to strongly rursiradiate ribbing.

IV. Conclusions:

The marine Triassic rocks of Nevada have long served as a renowned site for ichthyosaur fossils around the world. Most famously, the Luning Formation at BISP has fascinated scientists and the general public for decades. This study demonstrates that the potential for Late Triassic ichthyosaurs in Nevada does not begin and end at BISP. The nearby Pilot and Cedar Mountains both show promise for continued research on the Luning Formation and the unusual abundance of giants that are preserved in the formation. Excavations in the Pilot Mountains could be useful in unraveling the mysteries surrounding the monotaxic nature of BISP or show that the Luning Formation there is unique when compared to other geographically close outcroppings of the formation. The

study also outlines the need for further exploration in both of these mountain ranges and other areas that have yet to produce ichthyosaur fossils like the Garfield Hills. The upper member of the Luning Formation in the Pilot Mountains and Garfield Hills extends into the Middle Norian, an area with markedly little representation in the ichthyosaur fossil record.

The objectives of this study evolved throughout the completion of fieldwork for this thesis, but the primary goal was achieved. The presence of giant shastasaurid ichthyosaurs in the latest Triassic of North America, and in particular Nevada is no longer in question. This was proven by the discovery of a new semi-articulated skeleton of giant ichthyosaur affinity at Ferguson Hill, in the Gabbs Valley Range of Nevada. The specimen is distinctly ichthyosaurian in morphology and appears to have histological features that may be shared amongst the Late Triassic shastasaurids. The specimen is also exceptionally well constrained stratigraphically, providing a strong argument for its place as not only the youngest shastasaurid in North America, but also the youngest shastasaurid in the world.

V. Future Work

The Late Triassic marine strata of Nevada remain underexplored for vertebrates and in need of significant future study and excavation. The Pilot and Cedar Mountains are exceptionally rich in large ichthyosaur material, including some partially associated suites of bones, but collection has been very limited, and to date no major excavations have been undertaken. Future work locating high quality sites and excavating these sites could provide a greater understanding of how the Luning fauna changes across its

distribution and shine light on the unique traits seen most prominently at BISP. The negative results in the Garfield Hills do not disqualify the area as a potential ichthyosaur locality either. In their recent study of Luning Formation facies Fucelli et al. (2023) listed new localities for invertebrate fossils that could also have potential as sites for vertebrate exploration, and the upper member of the Luning in the Pilot Mountains shows promise for future exploration. Discovering an albeit limited locality in a small amount of surveying shows that the area has high potential for more vertebrate remains. With recent biostratigraphic controls clarifying the age of the member, vertebrate localities in the upper member in the Pilot Mountains fill in important gaps in our understanding of shastasaurid ichthyosaur history in the Late Triassic.

In the Gabbs Valley Range around New York Canyon, significant amounts of work are still to be done. NYC-21-A1 is an ongoing excavation that shows potential for a significant portion of the individual to be preserved. Excavations are planned to continue on this site for the foreseeable future. Outside of the NYC-21-A1 quarry, vertebrate remains are common enough to warrant significant efforts to locate more associated skeletons. The small pistosaur vertebrae mentioned in this study and the addition of other fossils located in the most recent field season demonstrate a variance in taxa and relative abundance of vertebrates unmatched by any other site in the Rhaetian and early Jurassic. Further work could turn New York Canyon into a world class site for the study of Triassic/Jurassic boundary marine reptiles.

VI. References

Alroy, J., 2010, The Shifting Balance of Diversity Among Major Marine Animal Groups: *Science*, v. 329, p. 1191–1194, doi:10.1126/science.1189910.

- Atkinson, J.W., and Wignall, P.B., 2019, How quick was marine recovery after the end-Triassic mass extinction and what role did anoxia play? *Palaeogeography, Palaeoclimatology, Palaeoecology*, v. 528, p. 99–119, doi:10.1016/j.palaeo.2019.05.011.
- Balini, M., Jenks, J.F., Martin, R., McRoberts, C.A., Orchard, M.J., and Silberling, N.J., 2015, The Carnian/Norian boundary succession at Berlin-Ichthyosaur State Park (Upper Triassic, central Nevada, USA): *Paläontologische Zeitschrift*, v. 89, p. 399–433, doi:10.1007/s12542-014-0244-2.
- Bardet, N., Falconnet, J., Fischer, V., Houssaye, A., Jouve, S., Pereda Suberbiola, X., Pérez-García, A., Rage, J.-C., and Vincent, P., 2014, Mesozoic marine reptile palaeobiogeography in response to drifting plates: *Gondwana Research*, v. 26, p. 869–887, doi:10.1016/j.gr.2014.05.005.
- Benton, M.J., 1995, Diversification and Extinction in the History of Life: *Science*, v. 268, p. 52–58, doi:10.1126/science.7701342.
- Blackburn, T.J., Olsen, P.E., Bowring, S.A., McLean, N.M., Kent, D.V., Puffer, J., McHone, G., Rasbury, E.T., and Et-Touhami, M., 2013, Zircon U-Pb Geochronology Links the End-Triassic Extinction with the Central Atlantic Magmatic Province: *Science*, v. 340, p. 941–945, doi:10.1126/science.1234204.
- Brown, L.S., 1986, Structure of the northern Cedar Mountains, west-central Nevada: A study utilizing balanced cross-sections and surface data: Houston, Texas, M.A. thesis, Rice University.
- Callaway, J.M., and Massare, J.A., 1989, *Shastasaurus altispinus* (Ichthyosauria, Shastasauridae) from the Upper Triassic of the El Antimonio district, northwestern Sonora, Mexico: *Journal of Paleontology*, v. 63, p. 930–939, doi:10.1017/S0022336000036635.
- Chen, Z.-Q., and Benton, M.J., 2012, The timing and pattern of biotic recovery following the end-Permian mass extinction: *Nature Geoscience*, v. 5, p. 375–383, doi:10.1038/ngeo1475.
- Clement, A.M., and Tackett, L.S., 2021, Facies stacking and distribution in the Gabbs Formation (Late Triassic, west-Central Nevada, U.S.A.): An environmental baseline to the end-Triassic carbonate crisis: *Sedimentary Geology*, v. 425, p. 106021, doi:10.1016/j.sedgeo.2021.106021.
- Cornwall, D.E., 1979, Paleoecology of Upper Triassic Bioherms in the Pilot Mountains, Mineral County, West-Central Nevada: Reno, Nevada, M.S. thesis, University of Nevada, Reno.

- Corso, J.D., Marzoli, A., Tateo, F., Jenkyns, H.C., Bertrand, H., Youbi, N., Mahmoudi, A., Font, E., Buratti, N., and Cirilli, S., 2014, The dawn of CAMP volcanism and its bearing on the end-Triassic carbon cycle disruption: *Journal of the Geological Society*, v. 171, p. 153–164, doi:10.1144/jgs2013-063.
- Crafford, A.E.J., 2007, *Geologic Map of Nevada: U.S. Geological Survey Data Series 249*, 1 CD-ROM, 46 p., 1 plate.
- Davies, J.H.F.L., Marzoli, A., Bertrand, H., Youbi, N., Ernesto, M., and Schaltegger, U., 2017, End-Triassic mass extinction started by intrusive CAMP activity: *Nature Communications*, v. 8, p. 15596, doi:10.1038/ncomms15596.
- Dick, D.G., and Maxwell, E.E., 2015, The evolution and extinction of the ichthyosaurs from the perspective of quantitative ecospace modelling: *Biology Letters*, v. 11, p. 20150339, doi:10.1098/rsbl.2015.0339.
- Firby, J. R., Schorn, H.E, and Lugaski, T.P., 1981, *Paleontological Inventory of the Carson City Bureau of Land Management District and paleontological bibliography of Nevada, volumes 1 & 2*. Unpublished report
- Fischer, V., Cappetta, H., Vincent, P., Garcia, G., Goolaerts, S., Martin, J.E., Roggero, D., and Valentin, X., 2014, Ichthyosaurs from the French Rhaetian indicate a severe turnover across the Triassic–Jurassic boundary: *Naturwissenschaften*, v. 101, p. 1027–1040, doi:10.1007/s00114-014-1242-7.
- Fröbisch, N.B., Fröbisch, J., Sander, P.M., Schmitz, L., and Rieppel, O., 2013, Macropredatory ichthyosaur from the Middle Triassic and the origin of modern trophic networks: *Proceedings of the National Academy of Sciences*, v. 110, p. 1393–1397, doi:10.1073/pnas.1216750110.
- Fucelli, A., Golding, M., Peybernes, C., and Martini, R., 2023, Siliciclastic input controlling carbonate deposition on a low-angle ramp system: New insight from the Upper Triassic Luning Formation (Western-Central Nevada): *Sedimentary Geology*, v. 450, p. 106394, doi:10.1016/j.sedgeo.2023.106394.
- Fujisaki, W., Fukami, Y., Matsui, Y., Sato, T., Sawaki, Y., and Suzuki, K., 2020, Redox conditions and nitrogen cycling during the Triassic-Jurassic transition: A new perspective from the mid-Panthalassa: *Earth-Science Reviews*, v. 204, p. 103173, doi:10.1016/j.earscirev.2020.103173.
- Fujisaki, W., Matsui, Y., Asanuma, H., Sawaki, Y., Suzuki, K., and Maruyama, S., 2018, Global perturbations of carbon cycle during the Triassic–Jurassic transition recorded in the mid-Panthalassa: *Earth and Planetary Science Letters*, v. 500, p. 105–116, doi:10.1016/j.epsl.2018.07.026.

- Greene, S.E., Martindale, R.C., Ritterbush, K.A., Bottjer, D.J., Corsetti, F.A., and Berelson, W.M., 2012, Recognising ocean acidification in deep time: An evaluation of the evidence for acidification across the Triassic-Jurassic boundary: *Earth-Science Reviews*, v. 113, p. 72–93, doi:10.1016/j.earscirev.2012.03.009.
- Guex, J., Bartolini, A., Atudorei, V., and Taylor, D., 2004, High-resolution ammonite and carbon isotope stratigraphy across the Triassic–Jurassic boundary at New York Canyon (Nevada): *Earth and Planetary Science Letters*, v. 225, p. 29–41, doi:10.1016/j.epsl.2004.06.006.
- Guex, J., Bartolini, A., Taylor, D., Atudorei, V., Thelin, P., Bruchez, S., Tanner, L., and Lucas, S., 2009, Comment on: “The organic carbon isotopic and paleontological record across the Triassic-Jurassic boundary at the candidate GSSP section at Ferguson Hill, Muller Canyon, Nevada, USA” by Ward et al. (2007): *Palaeogeography, Palaeoclimatology, Palaeoecology*, v. 273, p. 200–204, doi:10.1016/j.palaeo.2008.01.010.
- Gutarra, S., Moon, B.C., Rahman, I.A., Palmer, C., Lautenschlager, S., Brimacombe, A.J., and Benton, M.J., 2019, Effects of body plan evolution on the hydrodynamic drag and energy requirements of swimming in ichthyosaurs: *Proceedings of the Royal Society B: Biological Sciences*, v. 286, p. 20182786, doi:10.1098/rspb.2018.2786.
- Heimdal, T.H., Jones, M.T., and Svensen, Henrik.H., 2020, Thermogenic carbon release from the Central Atlantic magmatic province caused major end-Triassic carbon cycle perturbations: *Proceedings of the National Academy of Sciences*, v. 117, p. 11968–11974, doi:10.1073/pnas.2000095117.
- Hogler, J.A., 1992, Taphonomy and Paleoecology of *Shonisaurus popularis* (Reptilia: Ichthyosauria): *PALAIOS*, v. 7, p. 108, doi:10.2307/3514800.
- Holland, S.M., and Regan, A.K., 2020, A new, more accurate, and easier to use Jacob’s staff: *Journal of Sedimentary Research*, v. 90, p. 669–672, doi:10.2110/jsr.2020.003.
- Ji, C., Jiang, D.-Y., Motani, R., Rieppel, O., Hao, W.-C., and Sun, Z.-Y., 2016, Phylogeny of the Ichthyopterygia incorporating recent discoveries from South China: *Journal of Vertebrate Paleontology*, v. 36, p. e1025956, doi:10.1080/02724634.2015.1025956.
- Kear, B.P., Engelschiøn, V.S., Hammer, Ø., Roberts, A.J., and Hurum, J.H., 2023, Earliest Triassic ichthyosaur fossils push back oceanic reptile origins: *Current Biology*, v. 33, p. R178–R179, doi:10.1016/j.cub.2022.12.053.
- Kelley, N.P. et al., 2022, Grouping behavior in a Triassic marine apex predator: *Current Biology*, v. 32, p. 5398–5405.e3, doi:10.1016/j.cub.2022.11.005.

- Kelley, N.P., and Pyenson, N.D., 2015, Evolutionary innovation and ecology in marine tetrapods from the Triassic to the Anthropocene: *Science*, v. 348, p. aaa3716, doi:10.1126/science.aaa3716.
- Klein, N., A. Canoville, and A. Houssaye. 2019. Microstructure of Vertebrae, Ribs, and Gastralia of Triassic Sauropterygians—New Insights into the Microanatomical Processes Involved in Aquatic Adaptations of Marine Reptiles. *Anatomical Record* v. 302, p. 1770–1791.
- Korte, C., Ruhl, M., Pálffy, J., Ullmann, C.V., and Hesselbo, S.P., 2018, Chemostratigraphy Across the Triassic–Jurassic Boundary, *in* Sial, A.N., Gaucher, C., Ramkumar, M., and Ferreira, V.P. eds., *Geophysical Monograph Series*, Wiley, p. 183–210, doi:10.1002/9781119382508.ch10.
- Kosch, B.F., 1990, A revision of the skeletal reconstruction of *Shonisaurus popularis* (Reptilia: Ichthyosauria): *Journal of Vertebrate Paleontology*, v. 10, p. 512–514, doi:10.1080/02724634.1990.10011833.
- Larina, E., Bottjer, D.J., Corsetti, F.A., Thibodeau, A.M., Berelson, W.M., West, A.J., and Yager, J.A., 2021, Ecosystem change and carbon cycle perturbation preceded the end-Triassic mass extinction: *Earth and Planetary Science Letters*, v. 576, p. 117180, doi:10.1016/j.epsl.2021.117180.
- Laws, R.A., 1982, Late Triassic depositional environments and molluscan associations from west-central Nevada: *Palaeogeography, Palaeoclimatology, Palaeoecology*, v. 37, p. 131–148, doi:10.1016/0031-0182(82)90036-0.
- Lomax, D.R., De la Salle, P., Massare, J.A., and Gallois, R., 2018, A giant Late Triassic ichthyosaur from the UK and a reinterpretation of the Aust Cliff ‘dinosaurian’ bones (W. O. Wong, Ed.): *PLOS ONE*, v. 13, p. e0194742, doi:10.1371/journal.pone.0194742.
- Lucas, S.G., Taylor, D.G., Guex, J., Tanner, L.H., and Krainer, K., 2007, THE PROPOSED GLOBAL STRATOTYPE SECTION AND POINT FOR THE BASE OF THE JURASSIC SYSTEM IN THE NEW YORK CANYON AREA, NEVADA, USA: *New Mexico Museum of Natural History and Science Bulletin*, v. 40, p. 30.
- Martin, J., Vincent, P., Suan, G., Sharpe, T., Hodges, P., Williams, M., Howells, C., and Fischer, V., 2014, A mysterious giant ichthyosaur from the lowermost Jurassic of Wales: *Acta Palaeontologica Polonica*, doi:10.4202/app.00062.2014.
- Martindale, R.C., Bottjer, D.J., and Corsetti, F.A., 2012, Platy coral patch reefs from eastern Panthalassa (Nevada, USA): Unique reef construction in the Late Triassic: *Palaeogeography, Palaeoclimatology, Palaeoecology*, v. 313–314, p. 41–58, doi:10.1016/j.palaeo.2011.10.007.

- McElwain, J.C., Beerling, D.J., and Woodward, F.I., 1999, Fossil Plants and Global Warming at the Triassic-Jurassic Boundary: *Science*, v. 285, p. 1386–1390, doi:10.1126/science.285.5432.1386.
- McElwain, J.C., Wagner, P.J., and Hesselbo, S.P., 2009, Fossil Plant Relative Abundances Indicate Sudden Loss of Late Triassic Biodiversity in East Greenland: *Science*, v. 324, p. 1554–1556, doi:10.1126/science.1171706.
- McGowan, C., and Motani, R., 1999, A Reinterpretation of the Upper Triassic Ichthyosaur *Shonisaurus*: *Journal of Vertebrate Paleontology*, v. 19, p. 42–49.
- Moon, B.C., and Stubbs, T.L., 2020, Early high rates and disparity in the evolution of ichthyosaurs: *Communications Biology*, v. 3, p. 68, doi:10.1038/s42003-020-0779-6.
- Motani, R., 2009, The Evolution of Marine Reptiles: *Evolution: Education and Outreach*, v. 2, p. 224–235, doi:10.1007/s12052-009-0139-y.
- Motani, R., Jiang, D., Tintori, A., Ji, C., and Huang, J., 2017, Pre- versus post-mass extinction divergence of Mesozoic marine reptiles dictated by time-scale dependence of evolutionary rates: *Proceedings of the Royal Society B: Biological Sciences*, v. 284, p. 20170241, doi:10.1098/rspb.2017.0241.
- Muller, S.W., and Ferguson, H.G., 1936, Triassic and Lower Jurassic Formations of West Central Nevada: *Geological Society of America Bulletin*, v. 47, p. 241–252, doi:10.1130/GSAB-47-241.
- Nicholls, E.L., and Manabe, M., 2004, Giant ichthyosaurs of the Triassic—a new species of *Shonisaurus* from the Pardonet Formation (Norian: Late Triassic) of British Columbia: *Journal of Vertebrate Paleontology*, v. 24, p. 838–849, doi:10.1671/0272-4634(2004)024[0838:GIOTTN]2.0.CO;2.
- Oldow, J.S., 1981, Structure and stratigraphy of the Luning allochthon and the kinematics of allochthon emplacement, Pilot Mountains, west-central Nevada: *Geological Society of America Bulletin*, v. 92, p. 888, doi:10.1130/0016-7606(1981)92<888:SASOTL>2.0.CO;2.
- Oldow, J.S., 1984, Evolution of a late Mesozoic back-arc fold and thrust belt, northwestern Great Basin, U.S.A.: *Tectonophysics*, v. 102, p. 245–274.
- Oldow, J.S., and Dockery, H.A., 1993, Geologic map of the Mina quadrangle, Nevada: NBMG Field Studies Map 6.
- Oldow, J.S., and Meinwald, J.N., 1992, Geologic map of Bettles Well quadrangle, Nevada: NBMG Field Studies Map 1.

- Oldow, J.S., Satterfield, J.I., and Silberling, N.J., 1993, Jurassic to Cretaceous transpressional deformation in the Mesozoic marine province of the northwestern Great Basin, in Lahren, M.M., Trexler, J.H., Jr., and Spinosa, C., eds., *Crustal evolution of the Great Basin and Sierra Nevada: University of Nevada, Reno, Cordilleran/Rocky Mountain Section, Geological Society of America Guidebook*, p. 129–166.
- Padian, K., and Lamm, E.T., 2013, *Bone Histology of Fossil Tetrapods: Advancing methods, analysis, and interpretation: University of California Press*.
- Pálfy, J., and Kocsis, Á.T., 2014, Volcanism of the Central Atlantic magmatic province as the trigger of environmental and biotic changes around the Triassic-Jurassic boundary, *in* *Volcanism, Impacts, and Mass Extinctions: Causes and Effects*, Geological Society of America, doi:10.1130/2014.2505(12).
- Perillo, M., 2022, *GIANT SHADOWS IN THE LATE TRIASSIC SEA: Histological analysis on putative and genuine giant ichthyosaurs bone fragments: Bonn, Germany, M.S. thesis, Rheinische Friedrich-Wilhelms-Universität Bonn*.
- Percival, L.M.E., Ruhl, M., Hesselbo, S.P., Jenkyns, H.C., Mather, T.A., and Whiteside, J.H., 2017, Mercury evidence for pulsed volcanism during the end-Triassic mass extinction: *Proceedings of the National Academy of Sciences*, v. 114, p. 7929–7934, doi:10.1073/pnas.1705378114.
- Redelstorff, R., Sander, P.M., and Galton, P.M., 2012, Unique bone histology in partial large bone shafts from Aust Cliff (England, Upper Triassic): an early independent experiment in gigantism: *Acta Palaeontologica Polonica*, v. 59, p. 607–615, doi:10.4202/app.2012.0073.
- Renesto, S., Dal Sasso, C., Fogliazza, F., and Ragni, C., 2020, New findings reveal that the middle Triassic ichthyosaur *Mixosaurus cornalianus* is the oldest amniote with a dorsal fin.: *Acta Palaeontologica Polonica*, v. 65, doi:10.4202/app.00731.2020.
- Rigo, M. et al., 2020, The Late Triassic Extinction at the Norian/Rhaetian boundary: Biotic evidence and geochemical signature: *Earth-Science Reviews*, v. 204, p. 103180, doi:10.1016/j.earscirev.2020.103180.
- Rigo, M., Preto, N., Roghi, G., Tateo, F., and Mietto, P., 2007, A rise in the Carbonate Compensation Depth of western Tethys in the Carnian (Late Triassic): Deep-water evidence for the Carnian Pluvial Event: *Palaeogeography, Palaeoclimatology, Palaeoecology*, v. 246, p. 188–205, doi:10.1016/j.palaeo.2006.09.013.
- Ruhl, M., Hesselbo, S.P., Al-Suwaidi, A., Jenkyns, H.C., Damborenea, S.E., Manceñido, M.O., Storm, M., Mather, T.A., and Riccardi, A.C., 2020, On the onset of Central Atlantic Magmatic Province (CAMP) volcanism and environmental and carbon-

- cycle change at the Triassic–Jurassic transition (Neuquén Basin, Argentina): *Earth-Science Reviews*, v. 208, p. 103229, doi:10.1016/j.earscirev.2020.103229.
- Ruhl, M., and Kürschner, W.M., 2011, Multiple phases of carbon cycle disturbance from large igneous province formation at the Triassic–Jurassic transition: *Geology*, v. 39, p. 431–434, doi:10.1130/G31680.1.
- Ruhl, M., Kürschner, W.M., and Krystyn, L., 2009, Triassic–Jurassic organic carbon isotope stratigraphy of key sections in the western Tethys realm (Austria): *Earth and Planetary Science Letters*, v. 281, p. 169–187, doi:10.1016/j.epsl.2009.02.020.
- Sander, P.M., Chen, X., Cheng, L., and Wang, X., 2011, Short-Snouted Toothless Ichthyosaur from China Suggests Late Triassic Diversification of Suction Feeding Ichthyosaurs (L. Claessens, Ed.): *PLoS ONE*, v. 6, p. e19480, doi:10.1371/journal.pone.0019480.
- Sander, P.M., Griebeler, E.M., Klein, N., Juarbe, J.V., Wintrich, T., Revell, L.J., and Schmitz, L., 2021, Early giant reveals faster evolution of large body size in ichthyosaurs than in cetaceans: *Science*, v. 374, p. eabf5787, doi:10.1126/science.abf5787.
- Sander, P.M., Pérez de Villar, P.R., Furrer, H., and Wintrich, T., 2022, Giant Late Triassic ichthyosaurs from the Kössen Formation of the Swiss Alps and their paleobiological implications: *Journal of Vertebrate Paleontology*, p. e2046017, doi:10.1080/02724634.2021.2046017.
- van de Schootbrugge, B. et al., 2009, Floral changes across the Triassic/Jurassic boundary linked to flood basalt volcanism: *Nature Geoscience*, v. 2, p. 589–594, doi:10.1038/ngeo577.
- Silberling, N.J., 1959, Pre-Tertiary stratigraphy and Upper Triassic paleontology of the Union district, Shoshone Mountains, Nevada: Professional Paper USGS Numbered Series, 67 p.
- Silberling, N.J., 1991, Allochthonous terranes of Western Nevada, current status, in Raines, G.L., Lisle, R.E., Schafer, R.W., and Wilkinson, W.H., eds., *Geology and ore deposits of the Great Basin: Reno, Nev.*, Geological Society of Nevada, Symposium Proceedings, v. 1, p. 101–102.
- Stanley, G.D., 1979, PALEOECOLOGY, STRUCTURE, AND DISTRIBUTION OF TRIASSIC CORAL BUILDUPS IN WESTERN NORTH AMERICA: *The University of Kansas Paleontological Contributions*, v. 65, p. 70.

- Stubbs, T.L., and Benton, M.J., 2016, Ecomorphological diversifications of Mesozoic marine reptiles: the roles of ecological opportunity and extinction: *Paleobiology*, v. 42, p. 547–573, doi:10.1017/pab.2016.15.
- Tackett, L.S., and Bottjer, D.J., 2016, PALEOECOLOGICAL SUCCESSION OF NORIAN (LATE TRIASSIC) BENTHIC FAUNA IN EASTERN PANTHALASSA (LUNING AND GABBS FORMATIONS, WEST-CENTRAL NEVADA): *PALAIOS*, v. 31, p. 190–202, doi:10.2110/palo.2015.070.
- Tanner, L.H., Lucas, S.G., and Chapman, M.G., 2004, Assessing the record and causes of Late Triassic extinctions: *Earth-Science Reviews*, v. 65, p. 103–139, doi:10.1016/S0012-8252(03)00082-5.
- Taylor, D.G., Boelling, K., and Guex, J., 2000, The Triassic/Jurassic System Boundary in the Gabbs Formation, Nevada: *GeoResearch Forum*, v. 6, p. 225–236.
- Taylor, D., Guex, J., and Lucas, S.G., 2021, AMMONOIDS OF THE LATEST TRIASSIC GABBS FORMATION AT NEW YORK CANYON, MINERAL COUNTY, NEVADA: *New Mexico Museum of Natural History and Science Bulletin*, v. 82, p. 393–425.
- Taylor, D.G., Smith, P.L., Laws, R.A., and Guex, J., 1983, The stratigraphy and biofacies trends of the Lower Mesozoic Gabbs and Sunrise formations, west-central Nevada: *Canadian Journal of Earth Sciences*, v. 20, p. 1598–1608, doi:10.1139/e83-149.
- Thibodeau, A.M., Ritterbush, K., Yager, J.A., West, A.J., Ibarra, Y., Bottjer, D.J., Berelson, W.M., Bergquist, B.A., and Corsetti, F.A., 2016, Mercury anomalies and the timing of biotic recovery following the end-Triassic mass extinction: *Nature Communications*, v. 7, p. 11147, doi:10.1038/ncomms11147.
- Thorne, P.M., Ruta, M., and Benton, M.J., 2011, Resetting the evolution of marine reptiles at the Triassic-Jurassic boundary: *Proceedings of the National Academy of Sciences*, v. 108, p. 8339–8344, doi:10.1073/pnas.1018959108.
- Trotter, J.A., Williams, I.S., Nicora, A., Mazza, M., and Rigo, M., 2015, Long-term cycles of Triassic climate change: a new $\delta^{18}\text{O}$ record from conodont apatite: *Earth and Planetary Science Letters*, v. 415, p. 165–174, doi:10.1016/j.epsl.2015.01.038.
- Ward, P.D., Garrison, G.H., Williford, K.H., Kring, D.A., Goodwin, D., Beattie, M.J., and McRoberts, C.A., 2007, The organic carbon isotopic and paleontological record across the Triassic–Jurassic boundary at the candidate GSSP section at Ferguson Hill, Muller Canyon, Nevada, USA: *Palaeogeography, Palaeoclimatology, Palaeoecology*, v. 244, p. 281–289, doi:10.1016/j.palaeo.2006.06.042.

- Whiteside, J.H., Olsen, P.E., Eglinton, T., Brookfield, M.E., and Sambrotto, R.N., 2010, Compound-specific carbon isotopes from Earth's largest flood basalt eruptions directly linked to the end-Triassic mass extinction: *Proceedings of the National Academy of Sciences*, v. 107, p. 6721–6725, doi:10.1073/pnas.1001706107.
- Yager, J.A., West, A.J., Corsetti, F.A., Berelson, W.M., Rollins, N.E., Rosas, S., and Bottjer, D.J., 2017, Duration of and decoupling between carbon isotope excursions during the end-Triassic mass extinction and Central Atlantic Magmatic Province emplacement: *Earth and Planetary Science Letters*, v. 473, p. 227–236, doi:10.1016/j.epsl.2017.05.031.
- Zaffani, M., Jadoul, F., and Rigo, M., 2018, A new Rhaetian $\delta^{13}\text{C}_{\text{org}}$ record: Carbon cycle disturbances, volcanism, End-Triassic mass Extinction (ETE): *Earth-Science Reviews*, v. 178, p. 92–104, doi:10.1016/j.earscirev.2018.01.004.

Appendix 1

Fossil inventories from the Pilot Mountains and Gabbs Valley Range, comparative rib size measurements, and $\delta^{13}\text{C}_{\text{org}}$ sample data from the New York Canyon quarry.

Table 1: 2018-19 Pilot Mountains Specimen Inventory, UMNH.A.2022.14

Field Number	Taxon	Element
18M-1	<i>Shonisaurus sp.</i>	Vertebra
18M-2	<i>Shonisaurus sp.</i>	Vertebra
18M-4	Ichthyosauria	Rib
18M-3A	<i>Shonisaurus sp.</i>	Vertebra
18M-3B	Ichthyosauria	Rib
18M-5	<i>Shonisaurus sp.</i>	Verte
18M-6	<i>Shonisaurus sp.</i>	Vertebra
18M-10	<i>Shonisaurus sp.</i>	Paddle Element
18M-14	Ichthyosauria	Rib
18M-12	Ichthyosauria	Rib
18M-16	Vertebrata	Fragment
18M-15	<i>Shonisaurus sp.</i>	Paddle Element
18M3-7	Ichthyosauria	Fragment
18M3-10	<i>Shonisaurus sp.</i>	Girdle Element
18M3-11	Ichthyosauria	Rib
18M3-12	Ichthyosauria	Fragment
18M3-13	Ichthosauria	Rib
18M3-13	Ammonoidea	Body
18M3-15	Ichthosauria	Rib
18M4-1	<i>Shonisaurus sp.</i>	Girdle Element
18M4-2	<i>Shonisaurus sp.</i>	Girdle Element
18M5-1	Ichthyosauria	Rib
18M5-2	<i>Shonisaurus sp.</i>	Girdle Element
18M5-3	Ichthyosauria	Girdle Element
16M6-1	<i>Shonisaurus sp.</i>	Girdle Element
18C1	Ichthyosauria	Fragment
18C2-1	Vertebrata	Fragment
18C-2-2	Vertebrata	Fragment
18C-2-3	<i>Shonisaurus sp.</i>	Vertebra
18-C2-4	<i>Shonisaurus sp.</i>	Girdle Element
18-C2-5	<i>Shonisaurus sp.</i>	Mandible
18C2-1	<i>Shonisaurus sp.</i>	Vertebra
18C4	<i>Shonisaurus sp.</i>	Vertebra
18C6	Ichthyosauria	Vertebra

Table 1: Cont.

18C8	<i>Shonisaurus sp.</i>	Humerus or Coracoid
18C11	<i>Shonisaurus sp.</i>	Girdle Element

Table 2: 2021-22 Specimen Inventory, UMNH.A.2022.10 & UMNH.A.2022.38

Field Number	Taxon	Element
CC21-A3	Vertebrata	Indet.
NYC-21-A1-1	Ichthyosauria	Rib
NYC-21-A1-2	Ichthyosauria	Rib
NYC-21-A1-3	Ichthyosauria	Centrum
NYC-21-A1-4	Ichthyosauria	Rib
NYC-21-A1-5	Ichthyosauria	Rib
NYC-21-A1-6	Ichthyosauria	Rib
NYC-21-A1-7	Ichthyosauria	Rib
NYC-21-A1-8	Ichthyosauria	Rib
NYC-21-A1-9	Ichthyosauria	Rib
NYC-21-A1-10	Ichthyosauria	Rib
NYC-21-A1-11	Ichthyosauria	Indet.
NYC-21-A1-12	Ichthyosauria	Rib
NYC-21-A1-13	Ichthyosauria	Rib
NYC-21-A1-14	Ichthyosauria	Rib
NYC-21-A1-15	Ichthyosauria	Rib
NYC-21-A1-16	Ichthyosauria	Rib
NYC-21-A1-17	Ichthyosauria	Rib
NYC-21-A1-18	Ichthyosauria	Rib
NYC-21-A1-19	Ichthyosauria	Rib
NYC-21-A1-20	Ichthyosauria	Rib
NYC-21-A1-21	Ichthyosauria	Centrum
NYC-21-A1-22	Ichthyosauria	Rib
NYC-21-A1-23	Ichthyosauria	Rib
NYC-21-A1-24	Pistosauria	Vertebra
LST-18-1	Pistosauria	Vertebrae
NYC-21-A1-IV1	<i>Choristoceras</i>	Body
NYC-21-A1-IV2	<i>Choristoceras shoshonensis</i>	Body
NYC-21-A1-IV3	Invertebrata	Trace
NYC-21-A1-IV4	Bivalvia	Body
NYC-21-A1-IV5	Ammonoidea	Body
NYC-21-A1-IV6	Cephalopoda	Body
NYC-21-A1-IV7	Ammonoidea	Body
NYC-21-A1-IV8	Ammonoidea	Body
NYC-21-A1-Y2-1	Ichthyosauria	Rib
NYC-21-A1-Y2-3	Ichthyosauria	Rib

Table 2: Cont.

Field Number	Taxon	Element
NYC-21-A1-Y2-4	Ichthyosauria	Gastralia
NYC-21-A1-Y2-7	Reptilia	Long Bone
NYC-21-A1-Y2-8	Ichthyosauria	Vert
NYC-21-A1-Y2-9	Ichthyosauria	Rib
NYC-21-A1-Y2-11	Ichthyosauria	Rib
NYC-21-A1-Y2-12	Ichthyosauria	Paddle
NYC-21-A1-Y2-13	Osteichthyes	Vert
NYC-21-A1-Y2-14	Ichthyosauria	Rib
NYC-21-A1-Y2-15	Ichthyosauria	Rib
NYC-21-A1-Y2-16	Ichthyosauria	Rib
NYC-21-A1-Y2-17	Ichthyosauria	Rib
NYC-21-A1-Y2-18	Ichthyosauria	Rib
NYC-21-A1-Y2-19	Ichthyosauria	Rib
NYC-21-A1-Y2-20	Ichthyosauria	Rib
NYC-21-A1-Y2-21	Ichthyosauria	Rib
NYC-21-A1-Y2-22	Ichthyosauria	Rib
NYC-21-A1-Y2-23	Ichthyosauria	Rib
GAM22-1	Reptilia	Rib
NYC-21-A1-Y2-IV1	<i>Choristoceras shoshonensis</i>	Body
NYC-21-A1-Y2-IV2	<i>Choristoceras shoshonensis</i>	Body
NYC-21-A1-Y2-IV3	<i>Arcestes</i>	Body
NYC-21-A1-Y2-IV4	<i>Choristoceras shoshonensis</i>	Body
NYC-21-A1-Y2-IV5	Bivalvia & Belemnitida	Body
NYC-21-A1-Y2-IV6	Belemnitida	Body
NYC-21-A1-Y2-IV7	<i>Choristoceras shoshonensis</i>	Body
NYC-21-A1-Y2-IV8	<i>Choristoceras indet.</i>	Body
NYC-21-A1-Y2-IV9	<i>Arcestes</i>	Body
NYC-21-A1-Y2-IV10	Bivalvia	Body
NYC-21-A1-Y2-IV11	Bivalvia	Body

Table 3: Rib Diameter Measurements (cm)

Rib	Rib Head	Begin Shaft	Proximal Shaft	Midshaft	Distal End	Reference
NYC-21-A1-1	-	-	61.8	-	-	Pers. Obs.
NYC-21-A1-2	-	-		46	-	Pers. Obs.
Rib 1						
NYC-21-A1-2	-	-	52.5	-	-	Pers. Obs.
Rib 2						
NYC-21-A1-2	-	-	52.2	-	-	Pers. Obs.
Rib 3						
NYC-21-A1-5	-	-	-	46.1	-	Pers. Obs.
NYC-21-A1-7	-	-	73.1	57	-	Pers. Obs.
NYC-21-A1-8	-	-	-	44.1	-	Pers. Obs.
NYC-21-A1-13	-	-	52.7	-	-	Pers. Obs.
NYC-21-A1-14	-	-	59.8	-	-	Pers. Obs.
NYC-21-A1-15	-	-	59.6	-	-	Pers. Obs.
NYC-21-A1-17	-	-	55.1	-	-	Pers. Obs.
NYC-21-A1-18	-	-	50.6	-	-	Pers. Obs.
Fig. 9 in Nicholls and Manabe, 2004	130	100	65	50	110	Nicholls and Manabe, 2004
PIMUZ A-III 744	-	-	-	40	-	Sander et al., 2022
P88791 Bonenburg	-	-	-	50.3	-	Martin Sander Pers. Comm.
S. Breier rib Bonenburg	-	-	-	40	-	Martin Sander Pers. Comm.
PVL 1949	-	-	-	41	-	Fischer et al., 2014
BC Field Photo	115	-	75	-	-	Martin Sander Pers. Comm.
NSMLV A-5 R4(11)	-	-	-	42.2	-	Pers. Obs.
NSMLV A-5 L3 (15)	-	-	-	45.5	94.5	Pers. Obs.
NSMLV A-5 L5	-	-	-	48.2	-	Pers. Obs.
NSMLV A-5 R1	-	-	51.1	-	-	Pers. Obs.

Table 4: Organic Carbon Isotope Results

Field #	m.	wt.% N	2022 $\delta^{13}\text{C}_{\text{org}}$ (‰ vs. VPDB)	2023 $\delta^{13}\text{C}_{\text{org}}$ (‰ vs. VPDB)	wt.% C
21IP-1	0	0.06	-29	-	0.7
21IP-2	0.1	0.07	-28.8	-	0.6
21IP-3	0.15	0.08	-28.9	-	0.7
21IP-4	0.36	0.07	-28.8	-	0.5
21IP-5	0.52	0.05	-28.9	-	0.6
21IP-6	0.71	0.06	-28.7	-	0.3
21IP-7	0.93	0.06	-29	-	0.4
21IP-8	1.2	0.1	-29.2	-	0.6
21IP-9	1.7	0.06	-29	-29.6	0.5
SH-10(-20)	1.9	-	-	-29.8	-
SH-10(-10)	2	-	-	-30.18	-
21IP-10	2.1	0.05	-30.7	-31.125	0.5
SH-10	2.1	-	-	-30.765	-
SH-10(+10)	2.2	-	-	-31.115	-
21IP-10.1	2.21	0.05	-28.9	-29.37	0.4
SH-10(+20)	2.3	-	-	-29.33	-
21IP-10.2	2.43	0.07	-29.4	-	0.7
21IP-11	2.81	0.06	-28.7	-	0.5
21IP-12	3.36	0.03	-30.2	-	0.2
21IP-13	3.76	0.03	-29.2	-	0.2
21IP-14	4.16	0.03	-29.8	-	0.3
21IP-15	4.46	0.03	-29.8	-	0.2

Appendix 2:

Measured Stratigraphic Section of the top of the lower carbonate member of the Luning:

